

Mitigating Environmental Impact During Unexpected Loss of Claus Tail Gas Reheaters

Amber L. Hans, Craig J. Moody and Philip J. Oberbroeckling

LyondellBasell Houston Refining

Contacts: amber.hans@lyondellbasell.com, craig.moody@lyondellbasell.com,
philip.oberbroeckling@lyondellbasell.com

Christopher B. Lavery, Connor E. Deering, and Robert A. Marriott

Alberta Sulphur Research Ltd.

Contacts: rob.marriot@ucalgary.ca, cblavery@ucalgary.ca

Disclaimer

All information (“Information”) contained herein is provided without compensation and is intended to be general in nature. You should not rely on it in making any decision. LyondellBasell and Houston Refining, LP accepts no responsibility for results obtained by the application of this information, and disclaims liability for all damages, including without limitation, direct, indirect, incidental, consequential, special, exemplary or punitive damages, alleged to have been caused by or in connection with the use of this Information. LyondellBasell and Houston Refining, LP disclaims all warranties, including, but not limited to, the implied warranties of merchantability and fitness for a particular purpose, that might arise in connection with this information.

Introduction

Process safety management is an absolute necessity and core requirement within the entire chemical processing industry, including for sulfur recovery operations. Likewise, environmental performance and community impact continue to be core value areas as well. Not only does this require efforts to increase efficiencies during normal operations, but it also requires forethought to curtail the environmental impacts of unplanned disruptions to normal operating conditions. During these unplanned disruptions, the protective systems deployed often place process safety management and environmental protection layers at odds with one another, especially regarding shutdown systems for fired equipment. This situation presented itself at the LyondellBasell (LYB) Houston Refinery sulfur recovery facilities. With the LYB Goal Zero philosophy (a strive to have zero HSE incidents globally), traditional equipment reliability improvements to address increasing electrical power disruption problems were not going to be good enough. This led to the idea of utilizing the tail gas unit (TGU) in a non-conventional way to provide further mitigation of the environmental impact of these events. The necessary modifications to utilize this new concept were implemented in August 2022.

The LYB Houston Refinery (known internally as Houston Refinery Operations abbreviated “HRO”) is located on the Houston Ship Channel in Houston, Texas. HRO is a fully integrated, full conversion very heavy/sour refinery with a crude oil processing capacity of 268,000 barrels per

calendar day (BPCD). The HRO Sulfur Recovery Complex (SRC) has a nameplate capacity of 1372 long-ton of sulfur per day (LT/D), accomplished with three Claus units and two tail gas unit/thermal oxidizer trains. The permitted capacity is 1029 LT/D. A unique feature of the HRO SRC is it's 100% integration of the amine acid gas and sour water acid gas feed systems providing the ability to source feed to any of the Claus units. Likewise, the Claus units are 100% integrated with the tail gas systems providing the ability of all three Claus tail gas streams to be routed to either of the two TGUs or thermal oxidizers (see Figure 1). Note, both TGUs are hydrogenation/amine based technologies using principally Topsoe "low-temperature" catalyst (TK-220 in U-435 and a split bed of TK-222/TK-220 in U-440; see Figures 2 and 3 for the TGU reactor configurations) and utilizing natural gas combustion via HEC burners to provide "inline" heating and reducing gas generation (RGG).

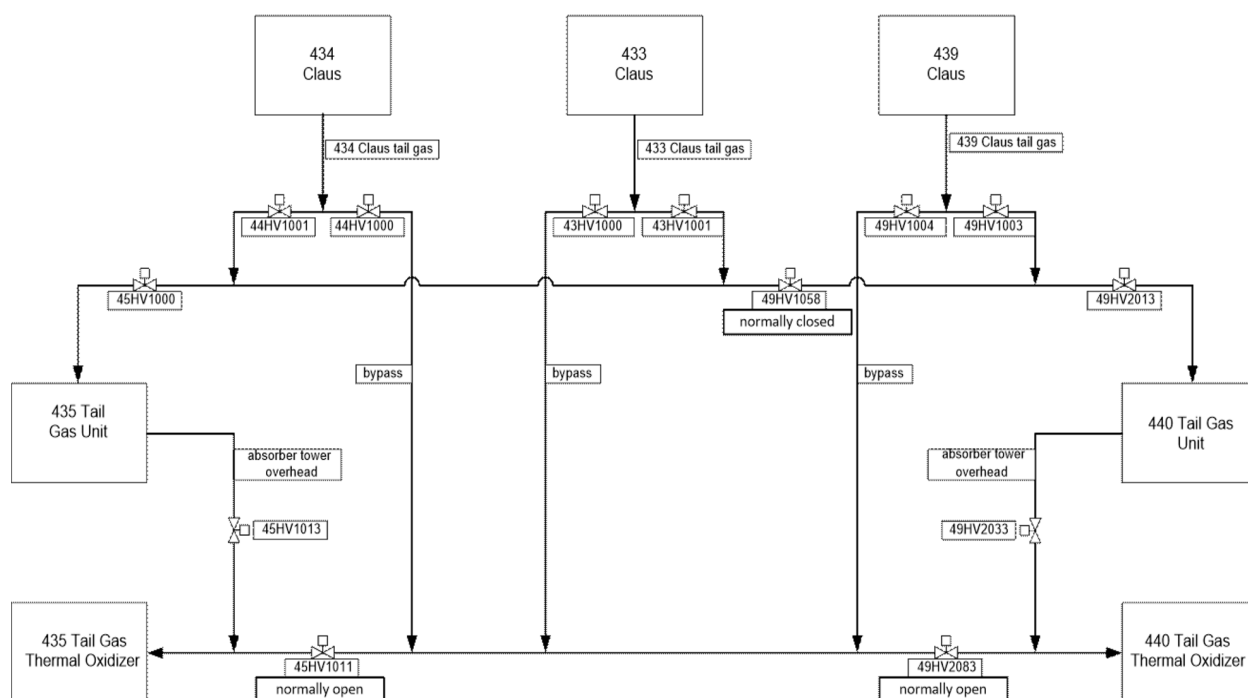


Figure 1: LYB Houston Refinery Claus Unit to Tail Gas Unit Gas Flow Path

435 SRU TAIL GAS REACTOR

CATALYST LOADING DIAGRAM

As Loaded August 2022

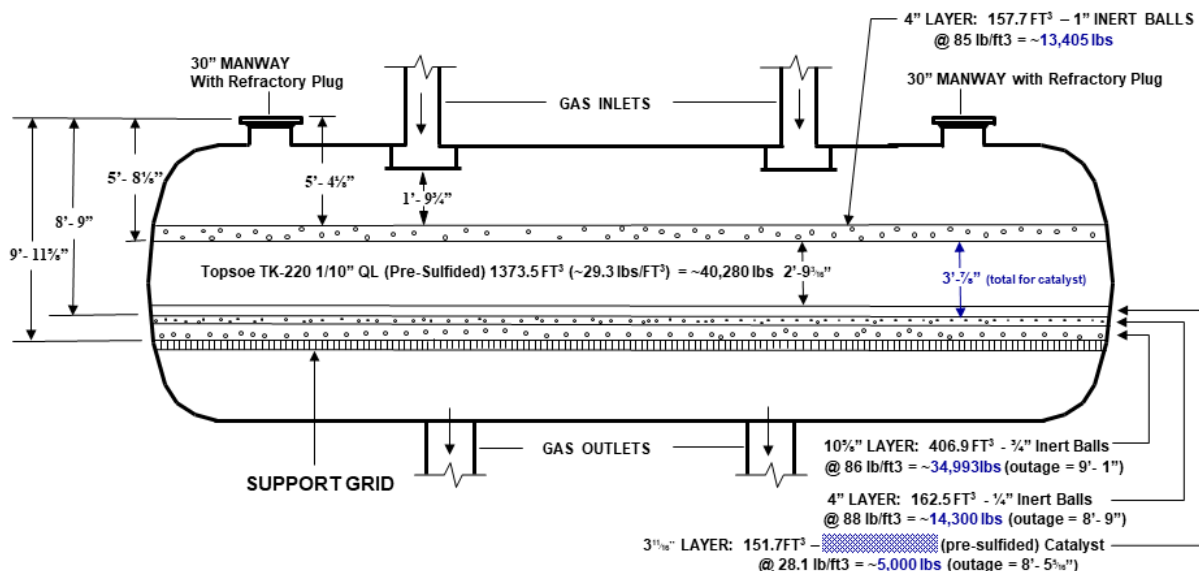


Figure 2: Catalyst loading diagram of the U-435 TGU at the HRO SRC.

440 TGU Hydrogenation Reactor (440R2001)

AS LOADED CATALYST LOADING DIAGRAM

May, 2019

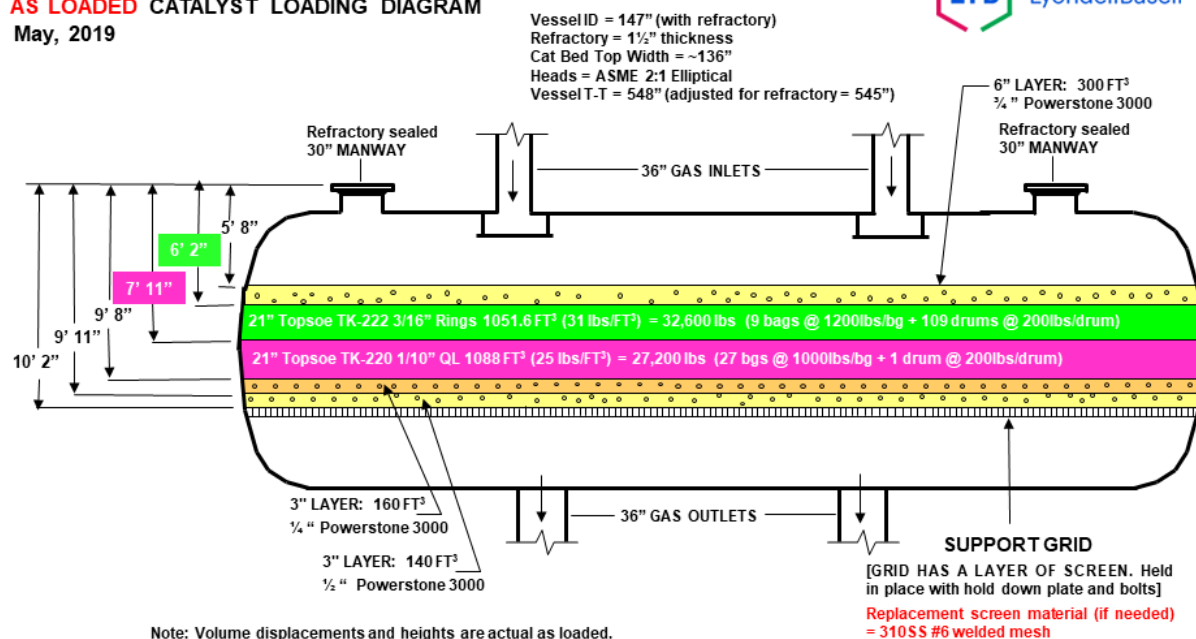


Figure 3: Catalyst loading diagram of the U-440 TGU at the HRO SRC.

Reliability and Environmental Incidents

As with any modified Claus process, the Claus units must have an operating TGU or thermal oxidizer available to safely process the tail gas in order for them to remain operational. Prior to the 2022 modifications, the Safety Instrumented Systems (SIS) protecting the sulfur recovery complex were designed to immediately and automatically divert Claus tail gas away from any of the TGU inline heaters and thermal oxidizers upon initiation of shutdown (*e.g.*, detection of loss of flame). Additionally, if the SIS logic determined that a viable tail gas path wasn't available (no flame in current routing and no flame or closed path for alternative routing), then a 2-minute delayed shutdown of the Claus Unit(s) would occur. Claus Unit acid gas feed inlet isolation valves then immediately close upon unit shutdown activation; thus, automatically routing acid gas to an elevated flare upon reaching the pressure controller set point.

Beginning in 2017, HRO began experiencing periodic momentary power disruptions caused by many different factors, many of which were not within LYB control. All but one of the eight air delivery blowers to the TGU inline heaters and thermal oxidizers are electric motor driven. When these power disruptions would occur, the corresponding TGU inline heaters and/or thermal oxidizer would trip off-line. Other factors could also contribute to trips of these units that were unrelated to the actual sulfur recovery process. Following each of these trip events, the automatic closing of the TGU feed inlet valve would have a sudden significant increase in gas load sent to the other operational TGU, which led to environmental excursions releasing sulfur dioxide from the thermal oxidizer. On other occasions the Claus tail gas would ultimately be diverted to the thermal oxidizer, adding to the emissions released. Other environmental releases would occur when the Claus Units tripped due to back pressure on the units resulting in acid gas being sent to the flare system. Each time, the operations team had to manually restart units and the refinery was forced to make sudden production cuts to mitigate the impact; and of course each upset resulted in an emission event.

The number of emission events and permit excursions were growing resulting in unacceptable reliability performance and contrary to the LYB Goal Zero philosophy. Numerous reliability projects aimed at achieving better on-line performance were implemented such as blower motor under voltage regulators, auto motor starters and thermal oxidizer continuous pilots. However, although providing marked improvement, none could ultimately deliver the level of reliability expected by the site. A true "silver bullet" was needed to make a solid step change in reliable on-line performance.

As a result, an idea was forged to aid the mitigation efforts. This involved a non-conventional approach to Claus tail gas management during these upsets. The idea centered on the concept that because the actual TGU reactors deployed in the units are very large, have significant mass in catalyst and inert grading, and have a heat barrier with the refractory lining, they emulate an adiabatic behavior with regard to system heat transfer. Thus, during a TGU ILH trip event where even though the tail gas feed temperature is reduced well below the necessary reaction temperature for sulfur species conversion to H_2S ; theoretically, heat transfer from the reactor mass and the corresponding exothermic reactions would for a period of time continue to maintain conditions necessary for the reactions to complete within the reactor catalyst bed. If viable, this would be the

“silver bullet” to significantly aid in achieving Goal Zero performance. However, proof of concept was needed to determine viability and to pass the necessary PSM hurdles for application. This is when the LYB team turned to Alberta Sulphur Research Ltd. (ASRL) to develop a research program to determine the viability of this idea.

The ASRL Study

A research program was designed to assess this non-conventional approach in responding to a loss of the tail gas reheaters for U-435 and U-440 (see Figure 1) at the HRO SRC. The strategy involves continuing to flow the process tail gas through the hydrogenation reactor while the catalyst bed is dropping in temperature during the ILH trip event. Consequently, the underlying concept of this approach relies on adequate catalyst performance (*i.e.*, no SO₂ breakthrough to the quench tower) at lower than typical bed inlet temperatures. Early research in this program was performed in an isothermal bench scale catalytic reactor system. During this initial testing it was found that even while operating for multiple hours at bed temperatures as low as 135°C/275°F (*i.e.*, temperature of the last condenser in the Claus Unit), no SO₂ breakthrough had occurred. However, it was determined that a significant portion of the SO₂ was participating in the Claus reaction to generate elemental sulfur on the catalyst surface. Fortunately, the sulfur formed was retained within the catalyst bed and could be reduced to H₂S for capture in the TGU amine unit upon returning to normal bed temperatures. Therefore, if the TGU reheaters could be restored in sufficient time, the net effect of this chemistry would be as if the power disruption had not occurred. Note that CS₂ and COS were not included as tail gas components in these studies, but it is expected that conversion of these species would suffer from lower temperatures.

To follow up on the promising findings obtained in the isothermal system, a novel adiabatic bench scale reactor was developed. Within the adiabatic reactor system: i) the temperature at which sulfur begins to form was confirmed, ii) the timing to reach this temperature after loss of the tail gas reheater was established, and iii) by comparing reaction exotherms within the catalyst bed before and after the temperature event, it could be verified that no detectable damage was done to the catalyst.

Experimental description:

An overview of the experimental system that was used in both the isothermal and adiabatic portions of this study is presented in Figure 4. Generally, the setup used consisted of an inlet manifold with individual mass flow controllers for regulating the flow of feed gases and an HPLC pump for delivering water. The liquid water was passed through a heated vaporizer prior to blending with the rest of the feed. Sulfur vapor was added to the feed by passing N₂ through the vapor phase of a heated reservoir containing liquid sulfur. Several checks were performed before and after each test to determine the concentration of sulfur, once combined with the entire feed.

During isothermal testing, a stainless steel fixed-bed reactor with dimensions of 1" OD × ¾" ID and overall length of 15½" was operated in a downward flow mode with temperature control to within ±1°C provided by a fluidized sand bath. Monitoring of the reactor temperature was performed through a series of axially mounted thermocouples located down the side of the reactor.

For these tests, the reactor was charged with 70 mL total of TK-220 (35 mL, bottom) and TK-222 (35 mL, top). For reasons that will be described later, after the gas sampling port, the reactor effluent was passed through transparent glass cold-water traps to precipitate any potential elemental sulfur present in the product stream for quantification (see Figure 5).

During adiabatic testing, the fixed-bed reactor was fabricated from borosilicate and had an ID of 1½" with an overall length of 20½" (Figure 6). A fraction of this overall length was contributed to by ¼" glass flanges that were added to either end of the reactor. The reactor was vacuum jacketed (2.5×10^{-6} Torr = 4.8×10^{-8} psi) and the inside of the vacuum jacket wall was mirror-coated with silver nitrate (AgNO₃). The vacuum jacket encompassed the entire length of reactor and the width of the annulus (*i.e.*, the space between the outside of the reactor wall and inside of the vacuum jacket wall) was 1". The adiabatic reactor was tied into the experimental system by horseshoe clamping 316 stainless steel flanges to the glass flanges at either end of the reactor (Figure 6). High-temperature soft silicone O-rings were used to create the seal between the glass and steel flanges. The steel flanges reduced to a 1½" OD and extended to 3½" in length. Each steel flange had an inner bore traversing their entire length that was sized appropriately to accommodate a ½" NPT fitting on the reduced end. The top steel flange was fitted with a reducing union that was connected to a ⅛" feed inlet line.

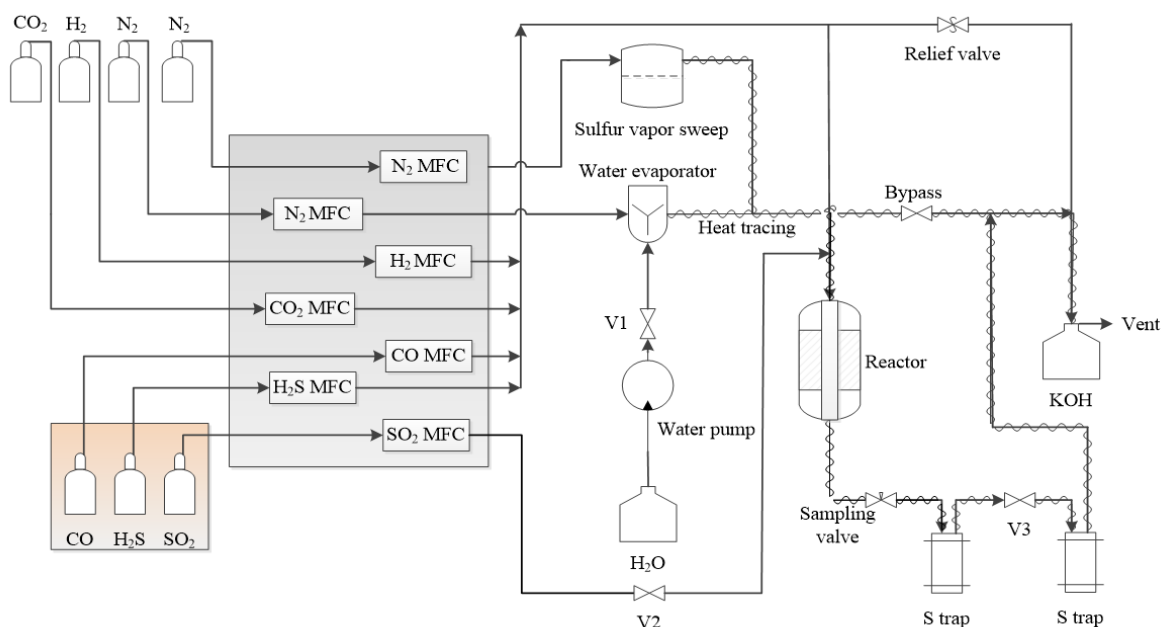


Figure 4: General overview of the experimental system. The main difference between the isothermal and pseudo-adiabatic systems was the reactor, for which the distinctions are described in the main body of the text.

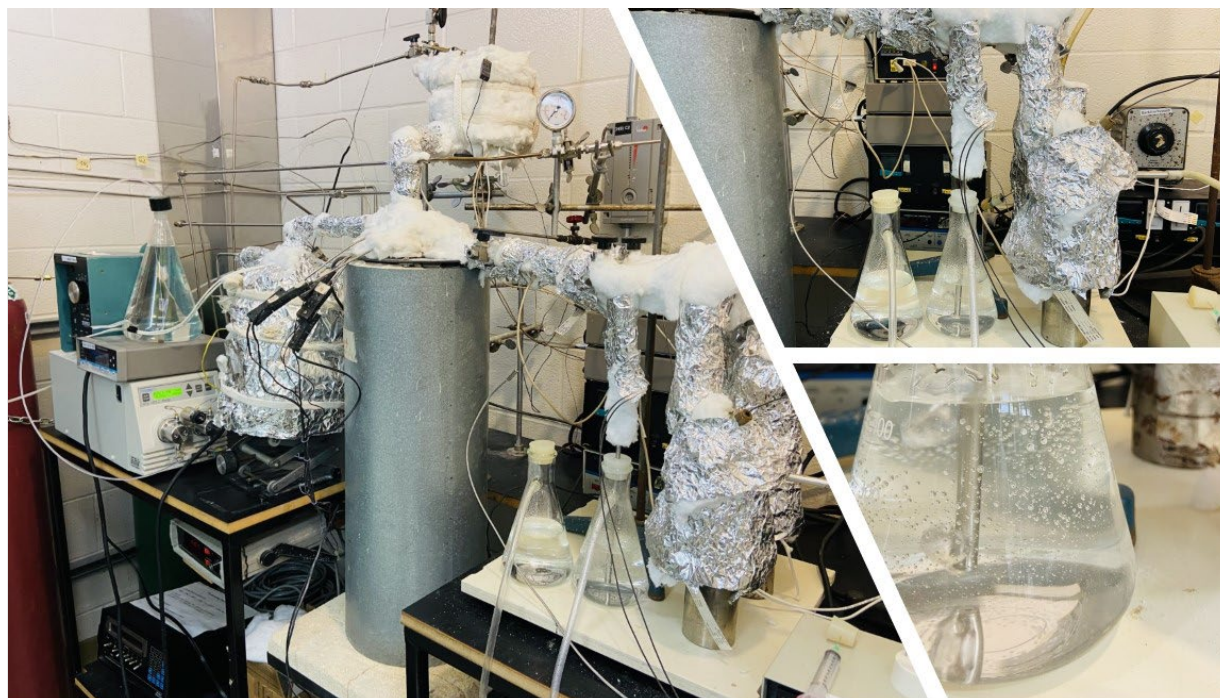


Figure 5: Photographs of the isothermal catalyst testing system showing the cold-water traps for sulfur precipitation.

The gas inlet temperature was controlled by adjusting the temperatures of the top steel flange and a coiled portion of the feed inlet line. The bottom flange was fitted with a $\frac{1}{2}$ " Tee that allowed for passage of the product gases to a sampling port and insertion of a thermocouple string for measuring bed temperatures. Heating the relatively large mass of the bottom steel flange also helped to minimize conductive heat loss from the main body of the reactor. The thermocouple string contained 32 thermocouples that were spaced by $\frac{1}{2}$ " to provide $15\frac{1}{2}$ " of temperature coverage. At its widest point, the thermocouple string had an OD of *ca.* $\frac{3}{8}$ " (*i.e.*, the width of 32 thermocouple guard columns bundled together) and at its most narrow point was *ca.* $\frac{1}{50}$ " in diameter (*i.e.*, the width of one thermocouple guard column). The thermocouples string was positioned within the center of the reactor and the catalyst (81.5 mL of TK-220 on bottom and 81.5 mL of TK-222 on top) was loaded around it. The overall length of the bed was *ca.* 12" and was positioned such that there were four thermocouples above the bed (in the feed gas), 24 thermocouples within the bed, and four thermocouples below the bed (in the effluent gas).

Despite the efforts described above to create a truly adiabatic system, while flowing just N_2 across the catalyst bed, some heat loss from the reactor was still observed. As such, 5 pseudo-adiabatic heat shields were added along the outside of the reactor, with a 6th on the outlet flange, (Figure 6) and turned on individually to see which thermocouples on the string responded the strongest. This determined which heat shield could be used to adjust a particular section of the bed. While flowing $2500 \text{ mL} \cdot \text{min}^{-1}$ of N_2 at inlet gas temperatures of 135, 150, 180, 210, 240, 270, and 300°C , the set points of each heat shield were adjusted until the temperature profile was constant throughout the reactor (*i.e.*, no net heat loss, Figure 7). This exercise produced calibrations which related the heatshield temperature required to keep each portion of the bed adiabatic across the experimental

temperature range. Due to the need for the heat shields to manifest no net heat loss from the system, the reactor is most accurately described as pseudo-adiabatic.

Prior to all testing, the tail gas catalyst samples were sulfided according to a procedure adapted from industry. This involved purging the catalyst with dry and O₂-free N₂ and then raising the temperature of the bed to 200°C/392°F. A sulfiding stream consisting of 2.0% (isothermal testing) or 2.5% (adiabatic testing) H₂S, 10.0% H₂ and 88.0% N₂ was then introduced, and the gas inlet temperature was slowly raised to *ca.* 315°C/599°F at an average rate of 7.5°C per 30 minutes. In the pseudo-adiabatic reactor, the ramp was adjusted accordingly to minimize any exotherm >30°C/50°F across the bed. Following the 8-hour temperature ramp, the catalyst was temperature-soaked at 315°C/599°F for a further 4 hours. The sulfiding stream was then shut off and replaced by dry O₂-free N₂ while the catalyst bed was adjusted to the appropriate experimental temperature for the testing described below.

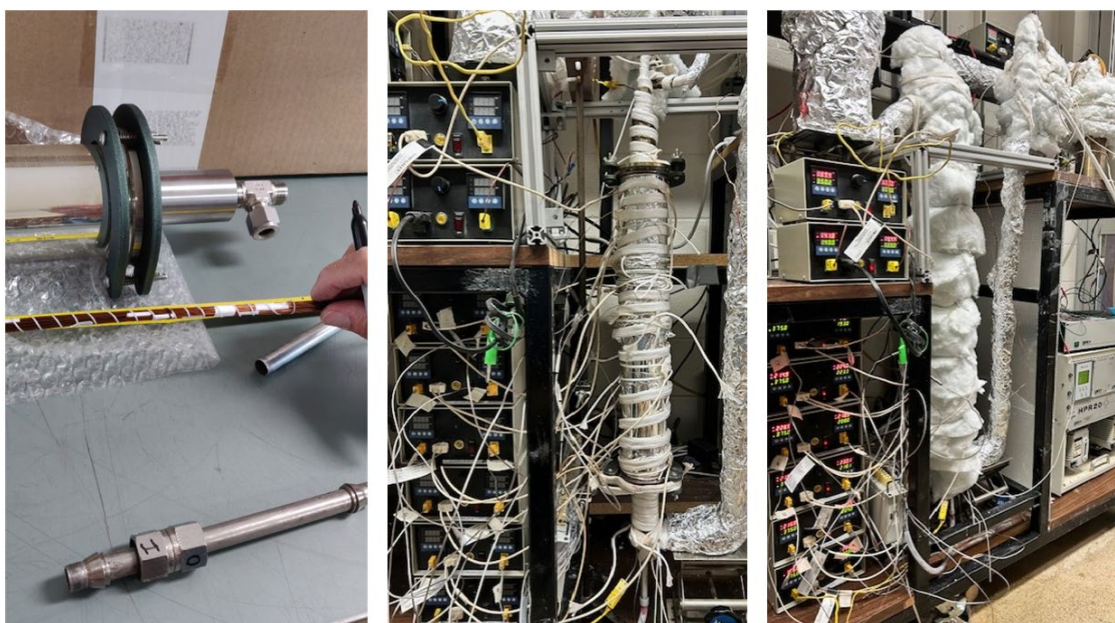


Figure 6: Photographs of the pseudo-adiabatic catalyst testing system showing the base of thermocouple string prior to insertion through bottom flange (left), mirrored and vacuum jacketed glass reactor with top and bottom steel flange attached and heat shields installed (center), and reactor fully insulated and tied into up- and down-stream portions of the system (right).

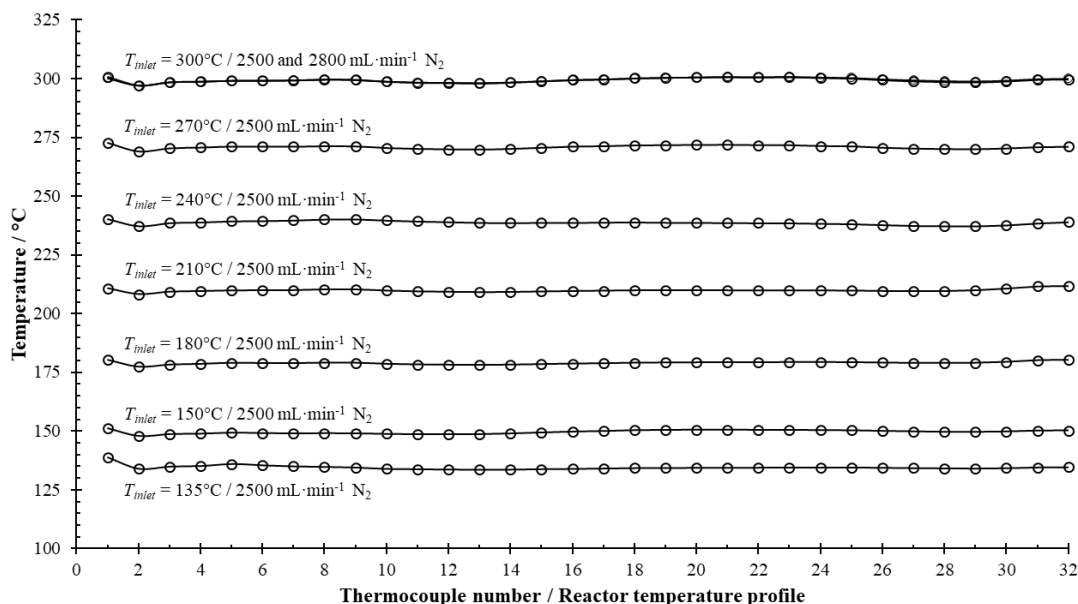


Figure 7: Plot showing the constant reactor temperature profiles achieved at various gas inlet temperatures during heat shield calibration.

Isothermal testing protocol. The target tail gas feed composition and conditions employed in the isothermal results discussed here are presented below.

(GHSV 675 h⁻¹, rel. to 20°C and 1 atm)

0.6%	H ₂ S
0.2%	SO ₂
2.5%	H ₂
0.3%	CO
1.8%	CO ₂
0.04%	S ₈
44.0%	H ₂ O
Bal.	N ₂

Samples of the reactor effluent were drawn every twenty-five minutes for gas chromatographic (GC) analysis. These gas samples were collected by manual withdrawal through a P₂O₅ cartridge to dry the stream and avoid loss of H₂S and potential SO₂ through the aqua-Claus reaction. Analysis for N₂, H₂S, SO₂, CO₂, CO, H₂, and any COS or CS₂ that could possibly be generated, was performed on a Varian 3800 gas chromatograph equipped with dual U-bond and Molsieve 5A columns connected to TCD and FID detectors.

Over the course of a 72-hour period, the catalyst bed temperature was cycled three times between the normal operating temperature ($T_{in} = 260^{\circ}\text{C}/500^{\circ}\text{F}$) and the last Claus condenser outlet temperature (135°C/275°F). Through mass balance calculations performed using GC results, any sulfur produced during time spent below normal operating temperature could be calculated. Then,

the excess H_2S that was measured upon resuming to normal operating temperature could be used to quantify how much sulfur was maintained on and within the catalyst pore structure during the temperature event. In addition to tracking elemental sulfur formation and retention on the catalyst through GC mass balance calculations, further efforts were made to quantify any sulfur slip from the bed. This was accomplished by passing the reactor effluent through transparent glass cold-water traps (see Figure 3) to precipitate any elemental sulfur present for filtering and weighing.

Pseudo-adiabatic testing protocol. The target tail gas feed composition and conditions employed in the adiabatic testing discussed here are presented below.

(GHSV 1200 h^{-1} , rel. to 20°C and 1 atm)

0.6%	H_2S
0.2%	SO_2
2.5%	H_2
0.3%	CO
1.8%	CO_2
0.04%	S_8
44.0%	H_2O
	Bal. N_2

Note that based on a Brimstone Report issued to Houston Refining in August of 2015, it is estimated that the above tail gas composition and GHSV correspond to a total sulfur load for U-433 +U-434+U-435 of *ca.* 625 LT/D.

Over the course of a 9-hour time frame: i) a stable baseline performance and temperature profile at a normal inlet temperature of $260^\circ\text{C}/500^\circ\text{F}$ was established, ii) the loss of the tail gas reheaters was simulated and the bed inlet temperature was allowed to drop until sulfur formation occurred, and then iii) the inlet gas temperature was raised back to $260^\circ\text{C}/500^\circ\text{F}$ for comparison to the baselines established at the beginning of the experiment. Through mass balance calculations performed using GC results, the amount of sulfur produced was calculated. Then, akin to the isothermal testing, the excess H_2S measured upon resuming to a $260^\circ\text{C}/500^\circ\text{F}$ inlet temperature was used to quantify how much sulfur was maintained on and within the catalyst pore structure during the power disruption simulation.

Laboratory results and discussion:

Isothermal testing. The GC data collected over the course of the 72-hour test are presented in Table A1 in the attached Appendix. From each set of GC results, the corresponding flowrate of H_2S ($\text{mmol}\cdot\text{min}^{-1}$) in the reactor effluent can be calculated. For comparison, these flowrates are also reported in Table A1 alongside the expected H_2S flowrates (based on conversion of all feed sulfur species to H_2S). Note that these H_2S flows (*i.e.*, expected versus measured) were used in the mass balance calculations that will be referenced later.

As a broad overview of the test, Figure 8 comprises a plot of measured product H_2S , expected product H_2S results (based on conversion of all feed sulfur species to H_2S), and bed temperature

versus time on stream. The overall test can be separated into three segments where the bed temperature was cycled back and forth between 260°C/500°F and 135°C/275°F at varying rates. Generally, with each drop in temperature, a point was reached where hydrogenation kinetics began to lag sulfur production from the Claus reaction on the catalyst support. This was manifested as a drop in product H₂S below the expected concentration. Notably, no SO₂ was detected in the reactor effluent throughout the entire duration of time on stream. Presumably, the SO₂ is largely taken to extinction by the Claus reaction at 135°C. Product H₂S levels never falling to 0.2 mols / 100 mols of feed (Table A1), however, suggest that some hydrogenation chemistry was still occurring, even at 135°C/275°F. Indeed, this threshold H₂S concentration would represent the Claus reaction consuming feed SO₂ to complete extinction and then no hydrogenation of either the feed or so-formed elemental sulfur. A more thorough description of the procedure and observations made during each of the temperature cycles is provided below.

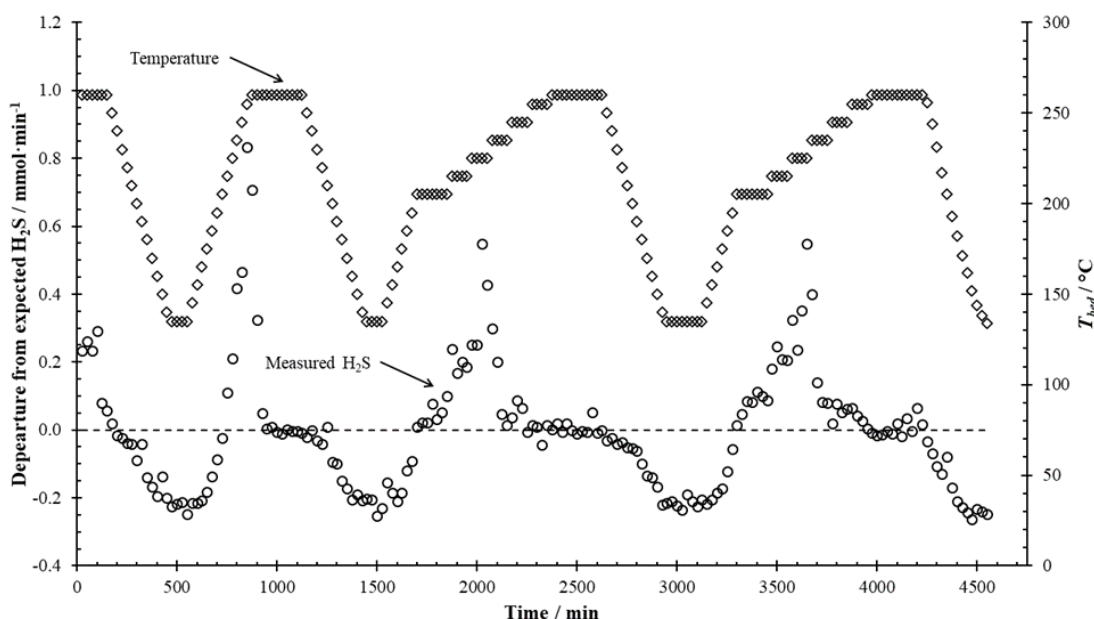


Figure 8: Temperature, expected H₂S, and measured H₂S versus time on stream during isothermal testing.

During Cycle 1 (0-1125 minutes / 0-18.8 hours), the tail gas feed was brought online until stable activity was observed and product H₂S levels were in line with expectations. At this point, after *ca.* 2 hours online, the first temperature swing was initiated with a 10°C decrease every 25 minutes; taking *ca.* 5.5 hours to reach 135°C/275°F. From Figure 6, sulfur production began to occur once the catalyst bed temperature dropped below the 205-210°C/400-410°F range. After being held at 135°C/275°F for *ca.* 1.3 hours, the temperature was increased back to 260°C/500°F at the same rate of 10°C per 25 minutes. From mass balance, a total of 2.5 g of elemental sulfur was formed until the temperature was raised back above the 205-210°C/400-410°F threshold, when a spike in product H₂S was observed. This spike in H₂S above expected levels lasted until after *ca.* 1 hour of operation back at a bed temperature of 260°C/500°F and corresponded to hydrogenation of the sulfur that was laid down on the catalyst during operation below 205-210°C/400-410°F. Interestingly, there was excellent agreement when comparing the total expected mols of H₂S in the

reactor effluent (Table 1, 353 mmol) over the course of Cycle 1 to what was measured (Table 1, 355 mmol). As mentioned above, these values can be calculated from the H_2S flowrates (mmol/min) reported in Table 1. In any event, this level of agreement indicates that the vast majority of sulfur formed during Cycle 1 was indeed retained on the catalyst and hydrogenated to H_2S upon resuming to temperatures $>205\text{--}210^\circ\text{C}/400\text{--}410^\circ\text{F}$. As shown in Figure 7, a very small amount of elemental sulfur was found in cold-water trap #4 which was attached to the system only once the reactor temperature had returned to $260^\circ\text{C}/500^\circ\text{F}$. This was quantified as a total of 0.03 g which represents a small fraction (1.2%) of the total 2.5 g that was formed, Table 2. The discrepancy between the two methods of determining sulfur slip from the catalyst bed can be attributed to some small, unavoidable experimental error.

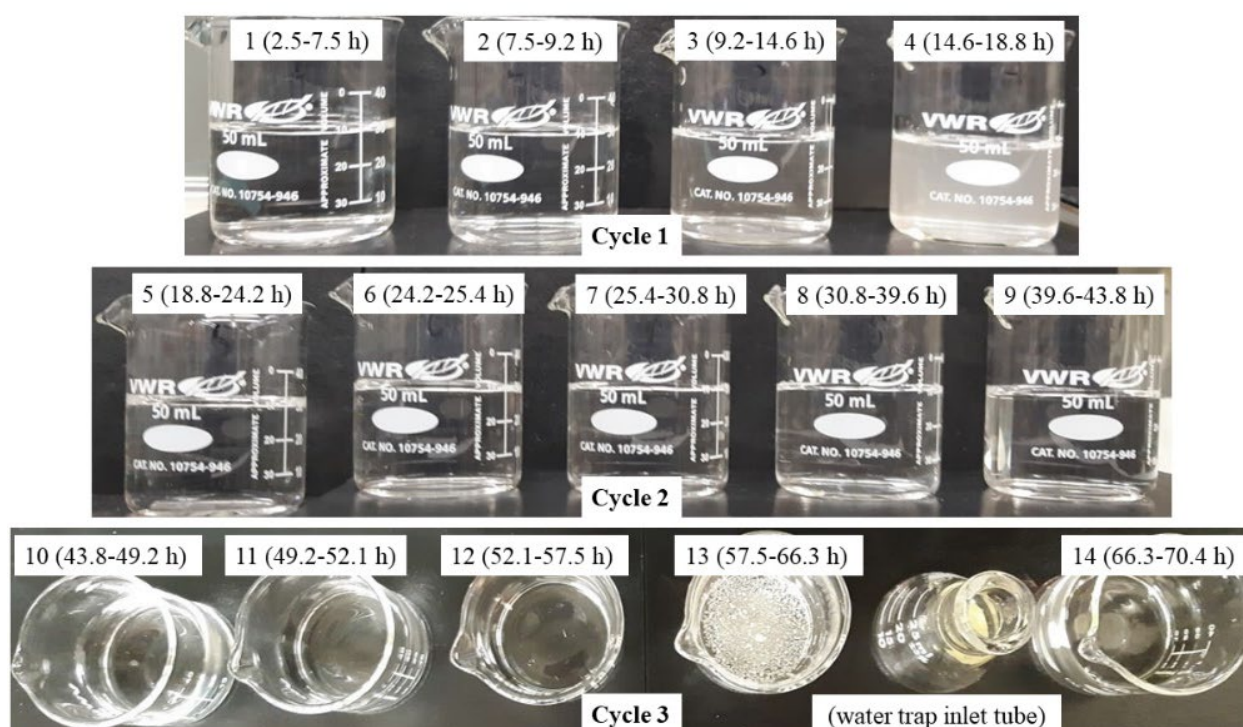


Figure 9: Comparison of the 14 different cold-water traps attached to the reactor outlet during various times of the three temperature cycles.

Procedurally, the only difference between Cycle 1 and Cycle 2 (1125-2625 minutes / 18.8-43.8 hours) was the rate at which the temperature was increased from $205^\circ\text{C}/400^\circ\text{F}$ to $260^\circ\text{C}/500^\circ\text{F}$. Where some sulfur was volatilized from the catalyst during Cycle 1 before it could be reduced, a slower approach was taken here (10°C per 75 minutes) in an attempt to fully hydrogenate the sulfur laid down before reaching $260^\circ\text{C}/500^\circ\text{F}$. In fact, with this tiered temperature program, the product H_2S spike had come back to expected levels during the temperature halt at $235^\circ\text{C}/455^\circ\text{F}$. As such, there was no sign of elemental sulfur detected in any of the cold-water traps during the entirety of Cycle 2 (Table 1 and Figure 9). Finally, as would be expected here, there was also excellent agreement when comparing the total expected mols of H_2S in the reactor effluent (Table 1, 543 mmol) over the course of Cycle 2 to what was measured (Table 1, 551 mmol).

Based on the success of Cycles 1 and 2, the procedure was adapted during Cycle 3 (2625-4225 minutes / 43.8-70.4 hours) to include additional sulfur formation. This was accomplished by increasing the time spent at 135°C/275°F from 75 minutes, as in Cycles 1 and 2, to 175 minutes. This procedural change resulted in a total of 3.5 g of elemental sulfur formation (Table 1). In following the same stepwise temperature ramp back to 260°C/500°F that was employed in Cycle 2, 0.1 g of elemental sulfur was collected in the downstream traps (Table 1). While this is more elemental sulfur than what was trapped in both Cycles 1 and 2, it still only represents 2.9% of total sulfur formation during Cycle 3. From the time stamps in Figure 9, it can be observed that most of this sulfur was collected between 205°C/401°F and 260°C/500°F and likely could have been reduced to H₂S with more time spent at 205°C/401°F.

Table 1: Comparisons of expected versus measured H₂S and elemental sulfur formed versus elemental sulfur trapped.

	Expected H ₂ S	Measured H ₂ S	Sulfur formed	Sulfur trapped
Cycle 1	353 mmol	355 mmol	2.5 g	0.03 g
Cycle 2	543 mmol	551 mmol	2.5 g	0.0 g
Cycle 3	579 mmol	584 mmol	3.5 g	0.1 g

Considering a tiered approach to restoring normal hydrogenation reactor temperature in the field may not be practical, deposition of too much elemental sulfur within the catalyst bed represents a practical limitation to this approach. However, the results above suggest that if a relatively small amount of sulfur is deposited, it should largely get reduced to H₂S upon returning to normal operating temperatures. Ideally, the power disruption could be resolved before the temperature drops to the point where sulfur formation begins. As will be discussed in the next section, this temperature, and the timing to reach this temperature, was further investigated under more representative field conditions in a reactor system that allowed us to simulate adiabatic conditions.

The BET surface areas and pore volumes of both fresh and used samples of TK-220 and TK-222 are presented in Table 2. In previous research, Al₂O₃ catalysts exposed to Claus conditions at similar temperatures were observed to have lost *ca.* 25-30% of their virgin surface area and *ca.* 20-25% of their virgin pore volume.[1] The used TK-220 was very much in line with these relative losses; suggesting that exposure to the 135°C conditions described above had no detrimental effect on the catalyst pore structure. Note that only *ca.* 10% of the virgin surface area of TK-222 was lost here.

Table 2: BET surface area and pore volume for fresh and used samples of TK-220 and -222.

	Fresh TK-220	Used TK-220	Fresh TK-222	Used TK-222
Surface Area / m²·g⁻¹	317.2	205.0	204.0	182.0
Pore Volume / cm³·g⁻¹	0.8	0.6	0.6	0.5

Similarly, the pore size distribution results suggest no harm was done to the catalyst during this testing. As mentioned above and can also be seen in Figures 10 and 11, there was a modest decrease in pore volume for the used samples which is typical upon exposure to Claus conditions at elevated temperatures. However, the relative distributions of pore sizes are analogous across all

comparisons, indicating no significant changes to the catalyst pore structures. This was also confirmed for macropores using mercury intrusion porosimetry.

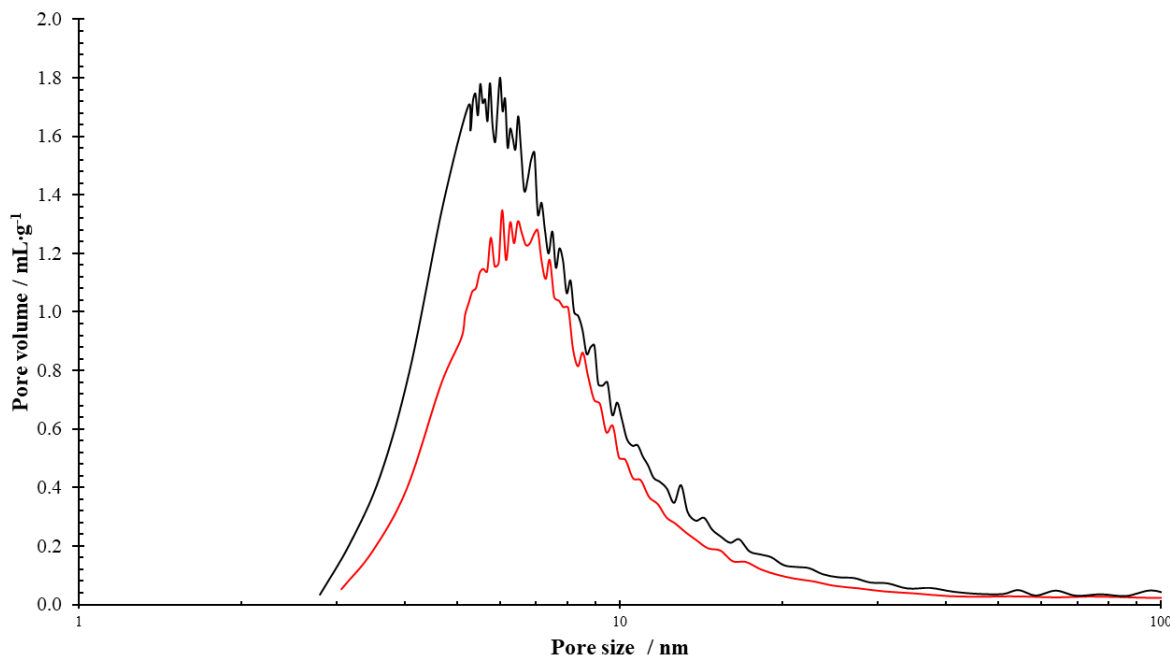


Figure 10: BJH pore size distribution for fresh (black) and used (red) TK-220.

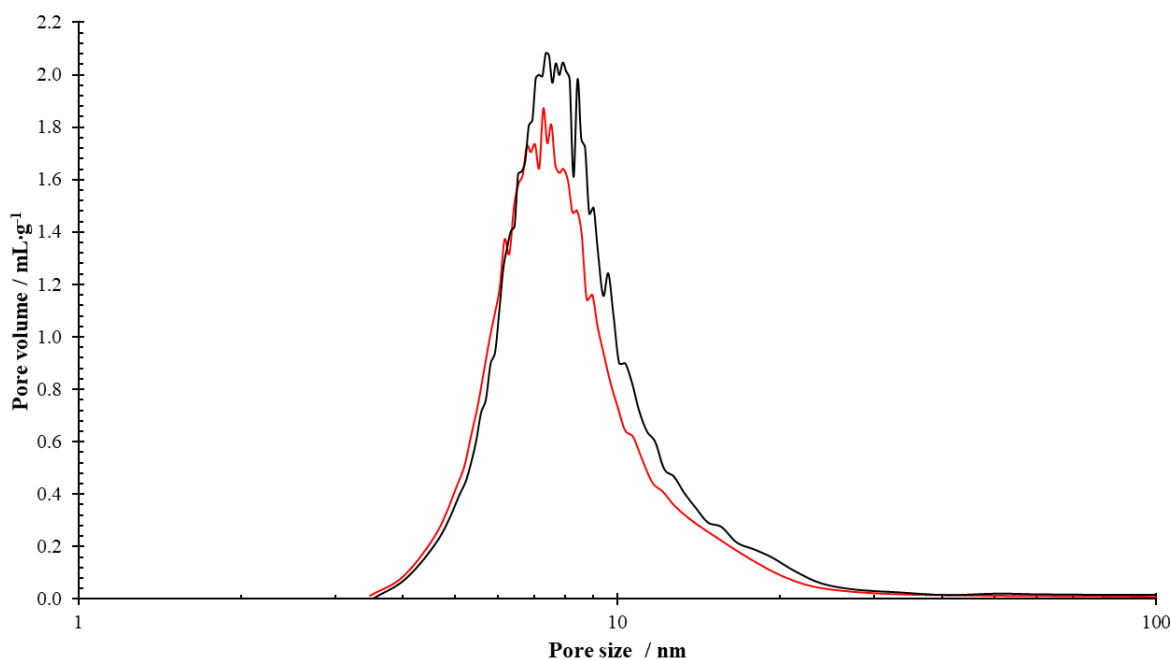


Figure 11: BJH pore size distribution for fresh (black) and used (red) TK-222.

Pseudo-adiabatic testing. As alluded to, the earlier phases of this research program were performed using an isothermal reactor (*i.e.*, reactor temperatures were achieved by use of an

electrically heated and air ebulliated sand-bath). However, during this last phase of testing, Houston Refining requested ASRL use an adiabatic reactor to generate results that could be applied more directly to a TGU in the field. More specifically, Houston Refining was interested in analyzing the rate of cooling within the adiabatic reactor upon switching from a normal operating gas inlet temperature of *ca.* 260°C/500°F to 135°C/275°F (*i.e.*, when simulating loss of the tail gas reheaters). Given the significance of the implications, Houston Refining also wanted to confirm the temperature at which net sulfur production begins within a reactor system simulating adiabatic conditions. Finally, performance before and after simulating the power disruption was to be further investigated to ensure no irreparable damage to the catalyst. Where laboratory experiments are overwhelmingly carried out in an isothermal system,[2] the fabrication of a functioning adiabatic reactor was a first for ASRL and considered a significant research accomplishment. Indeed, literature reporting on the successful implementation of bench scale reactors simulating adiabatic conditions is scarce [3-7]. The details of the newly fabricated adiabatic reactor are described in the experimental section and the deeper understanding it was able to add to this research is discussed below.

While the catalyst sulfiding procedure was not the focal point of this study, some general observations that were made while performing this exercise with the new reactor are worth noting. Over the course of the first 2.5 hrs, a clear reaction exotherm could be observed traversing from the top of the bed through to the bottom. At its largest point, the exotherm was *ca.* 30°C/55°F above the reactor inlet temperature. Once the exotherm had passed through the bed, the temperature profile was flatter and increased in accordance with the gas inlet temperature. The temperature profile of the catalyst bed at various points in time during sulfiding is shown in Figure 12.

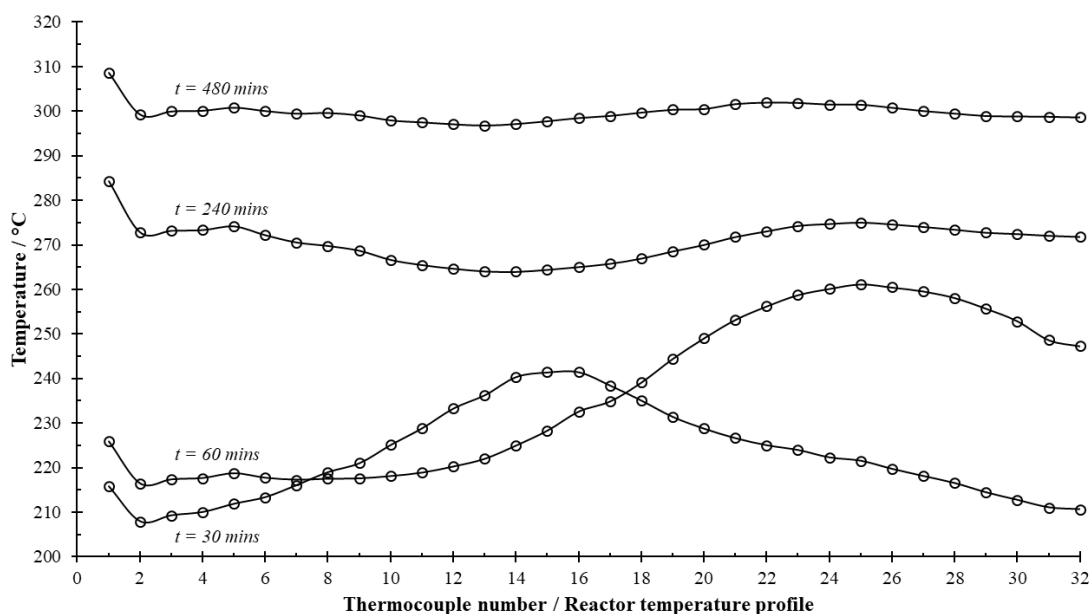


Figure 12: Temperature profile of catalyst bed at various times during catalyst sulfiding.

The GC data collected throughout the test simulating the loss and restoration of power to the tail gas reheater are presented in Table 3. A visual summary of the test results is also shown in Figure 13 where product H_2S , reactor inlet temperature, and reactor outlet temperature are all plotted against time on stream. During the first 197 minutes on stream, a stable exotherm was established and the product H_2S was measured while the reactor inlet temperature was at $260^\circ\text{C}/500^\circ\text{F}$ (*i.e.*, normal reheater operation). The product H_2S measured during this time was used to determine the baseline level and associated 95% confidence interval during normal operation. At the 197-minute mark, loss of the reheater was simulated and the gas preheat temperature was adjusted to $135^\circ\text{C}/275^\circ\text{F}$. As can be seen in Figure 13, this caused the reactor inlet temperature to begin dropping immediately. However, the first H_2S measurement to fall outside of one standard deviation below the baseline was not until the 250-minute mark. This drop in product H_2S represents the point at which hydrogenation kinetics begin to lag sulfur production from the Claus reaction which becomes more facile at lower temperatures. This measurement at 250 minutes was the first sample where the reactor inlet temperature fell below the $205\text{--}210^\circ\text{C}/400\text{--}410^\circ\text{F}$ temperature range. In reality, sulfur production likely began sometime between the samples taken at the 235- and 250-minute mark. This represents a 38 to 53 minute window between loss of the tail gas reheater and sulfur production on the catalyst surface. Note the sample taken at 250 minutes was also the first measurement taken after the reactor outlet temperature began to drop.

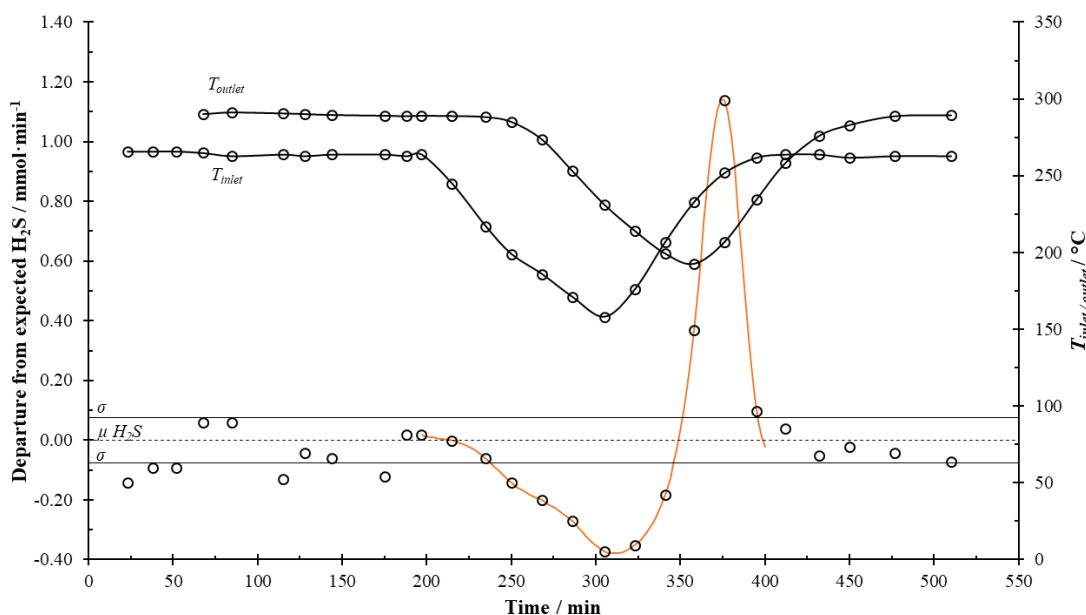


Figure 13: Temperature, expected H_2S , and measured H_2S versus time on stream. The orange line represents where the H_2S areas were integrated, μ is the baseline average (based on a longer time stream than shown), and σ represents the 95% confidence interval.

During the timeframe when the reactor inlet temperature was decreasing, an increase in CO was observed from loss in the water gas shift reaction (WGSR). While this would coincide with less H_2 formation, no real change in product H_2 concentration was observed due to less consumption of the feed H_2 .

Table 3: GC data collected while using the pseudo-adiabatic reactor and simulating loss and restoration of the tail gas reheaters.

Time (min.)	T_{inlet} (°C)	N ₂	H ₂ S	SO ₂	CO ₂	CO	H ₂	H ₂ O	S ₈	Outlet H ₂ S / mmol·min ⁻¹
		mols / 100 mols of feed								
<i>Feed</i>		<i>50.65</i>	<i>0.56</i>	<i>0.20</i>	<i>1.80</i>	<i>0.25</i>	<i>2.52</i>	<i>44.01</i>	<i>0.01</i>	
23	266	50.65	0.73	0.00	1.94	0.01	2.03	41.80	0.02	1.05
38	266	50.65	0.77	0.00	2.40	0.01	2.13	45.41	0.01	1.10
52	266	50.65	0.77	0.00	1.97	0.01	2.19	45.37	0.01	1.10
68	265	50.65	0.87	0.00	2.15	0.01	2.37	45.30	0.00	1.25
85	263	50.65	0.87	0.00	1.97	0.01	2.38	45.47	0.00	1.25
115	264	50.65	0.74	0.00	1.94	0.01	2.10	46.04	0.01	1.06
128	263	50.65	0.80	0.00	2.09	0.01	2.25	45.35	0.01	1.15
144	264	50.65	0.79	0.00	1.94	0.01	2.38	45.35	0.01	1.13
175	264	50.65	0.75	0.00	1.92	0.01	2.21	45.94	0.01	1.07
188	263	50.65	0.84	0.00	2.14	0.01	2.34	45.40	0.00	1.21
197	264	50.65	0.84	0.00	1.95	0.01	2.33	45.63	0.00	1.21
215	245	50.65	0.83	0.00	1.94	0.01	2.34	45.62	0.00	1.19
235	217	50.65	0.79	0.00	1.94	0.01	2.25	45.82	0.01	1.13
250	199	50.65	0.73	0.00	1.94	0.01	2.30	45.63	0.02	1.05
268	186	50.65	0.69	0.00	1.94	0.01	2.34	45.71	0.02	0.99
286	171	50.65	0.64	0.00	1.82	0.02	2.42	45.76	0.03	0.92
305	158	50.65	0.57	0.00	1.87	0.04	2.45	45.94	0.04	0.82
323	176	50.65	0.59	0.00	1.89	0.06	2.53	45.90	0.03	0.84
341	207	50.65	0.71	0.00	1.89	0.05	2.28	46.17	0.02	1.01
358	233	50.65	1.08	0.00	1.96	0.03	1.96	45.68	-0.03	1.56
376	252	50.65	1.62	0.00	1.93	0.01	1.36	45.12	-0.10	2.33
395	262	50.65	0.90	0.00	1.96	0.01	2.17	43.96	-0.01	1.29
412	264	50.65	0.86	0.00	1.94	0.01	2.23	45.42	0.00	1.23
432	264	50.65	0.80	0.00	1.92	0.01	2.15	45.67	0.01	1.14
450	262	50.65	0.81	0.00	1.94	0.01	2.29	45.38	0.00	1.17
477	263	50.65	0.80	0.00	1.94	0.01	2.49	45.43	0.01	1.15
510	263	50.65	0.78	0.00	1.94	0.01	2.15	46.14	0.01	1.12

At the 305-minute mark (1.8 hours after the reheater loss was simulated), the gas preheat temperature was adjusted back to 260°C/500°F and, as expected the reactor inlet temperature immediately started to increase. However, there was a 36-minute lag until the reactor outlet temperature began to increase as well. Regardless, as the reactor inlet temperature passed back through the 205-210°C/400-410°F range, a large spike in product H₂S was observed (Figure 13). As described in the isothermal section, this roll-up in H₂S, beyond expected levels based on the feed, corresponds to the hydrogenation of sulfur laid down while simulating loss of the tail gas reheater. Indeed, a significant drop in product H₂, below normal operation levels, was observed during the timing of this H₂S roll-up. Where portions of the bed were still below normal operating

temperatures here, some continued loss of the WGSR may have also been contributing to the relatively lower product H_2 levels (*i.e.*, increased consumption and decreased production).

For each set of GC results, the corresponding flowrate of H_2S ($mmols \cdot min^{-1}$) in the reactor effluent was calculated (Table 3). By integrating the area generated between the curves showing the drop in measured H_2S and the expected level of H_2S (Figure 13), the amount of elemental sulfur (S_8) deposited on the catalyst during testing was calculated to be 0.90 g. Similarly, it can be determined that the spike in H_2S beyond expected levels (Figure 13) corresponds to the hydrogenation of 0.94 g of elemental sulfur (S_8). The small discrepancy between these two numbers can be attributed to unavoidable experimental error. More data points to better define the H_2S curves above and below expected levels would likely bring these numbers closer together.

Snapshots of the stabilized temperature profile across the catalyst bed before and after the temperature event are presented in Figure 14. As shown, the before and after temperature profiles are indistinguishable; thus, indicating no damage to the catalyst from the lower-than-normal temperature of operation and resulting deposition of elemental sulfur.

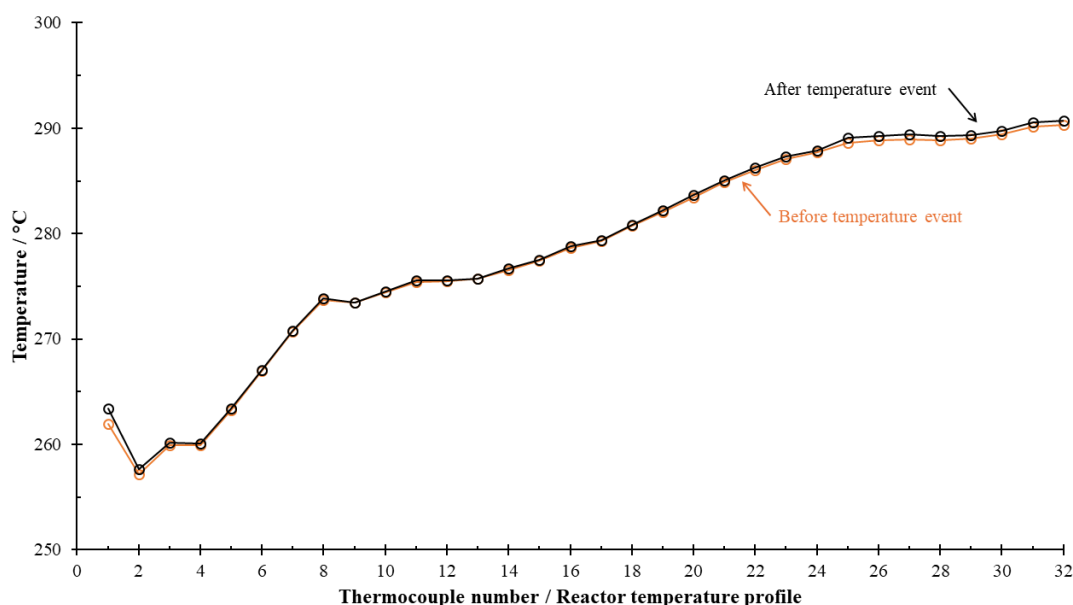


Figure 14: The stable temperature profile of the reaction during normal operation (260°C inlet), before and after the temperature event.

On inspection, the temperature profile during normal operation consists of three segments: (i) a relatively steep slope spanning thermocouple numbers 5-8, (ii) a relatively less steep slope that spans thermocouples 9-24, and (iii) a plateau from thermocouples 25-32. Presumably, the steepest slope in segment (i), which corresponds to the first 2" of the bed (*ca.* 17% of the bed), represents the heat of reaction arising from hydrogenation of the feed SO_2 and elemental sulfur, and the WGSR. The less steep slope in segment (ii) that extends 10" into the bed (*ca.* 83% of the bed) represents continued WGSR while the plateau across segment (iii), which encompasses the last 2" of the bed, corresponds to equilibrium.

Finally, during the downswing of the temperature event, the slopes in segment (i) and (ii) became more similar and appeared to span the entire bed (*i.e.*, no plateau in temperature observed, Figure 15). This would be in line with catalyst bed operating in the kinetic regime (*i.e.*, the reaction scheme in segment (i) was occurring across its entire length). This also matches with the previously mentioned changes in the outlet gas stream gas speciation.

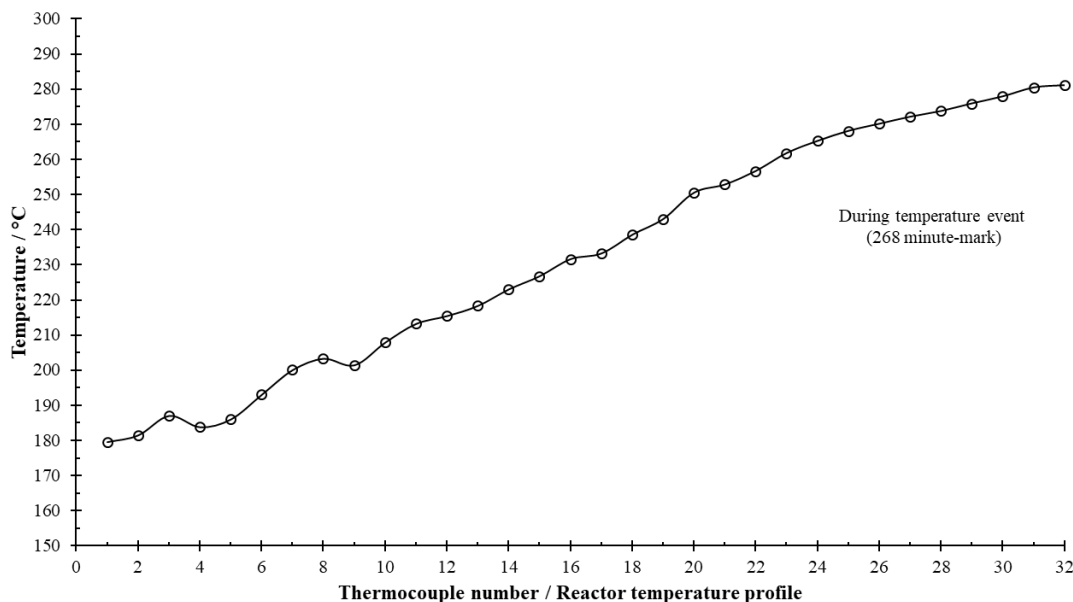


Figure 15: Reactor temperature profile at 268-minute when the bed outlet temperature began to drop.

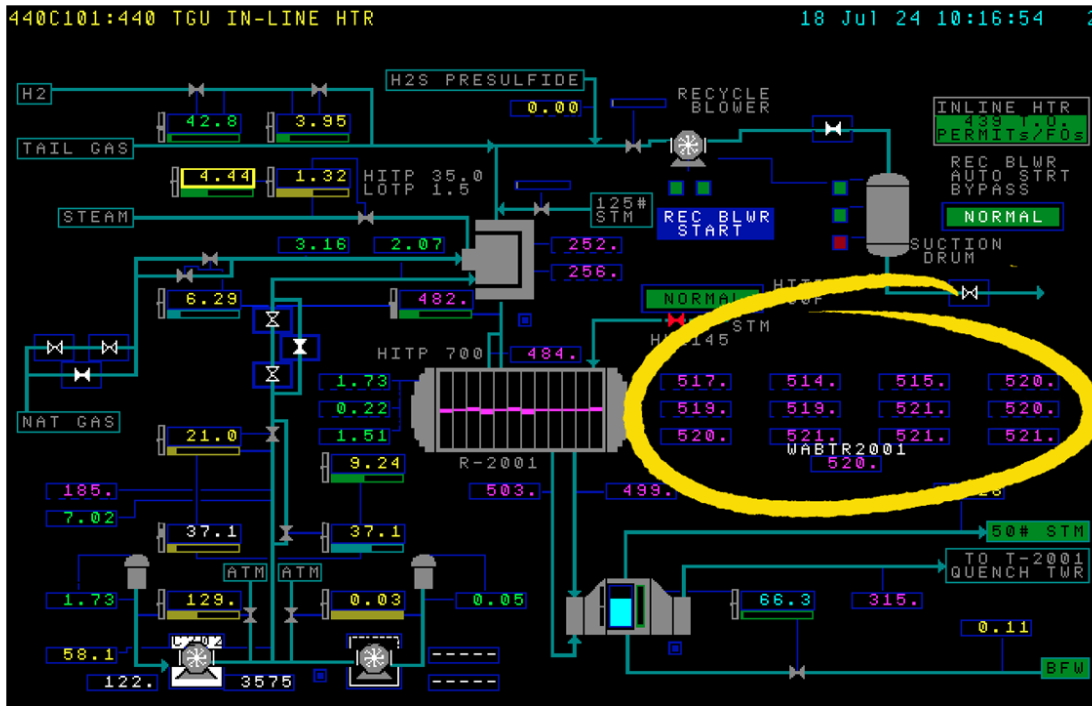
Summary of laboratory investigations:

The findings from both the isothermal and adiabatic studies were largely in line. The adiabatic studies further demonstrated that catalyst TK-220/222 can successfully operate (*i.e.*, no SO₂ breakthrough) at sub-dewpoint conditions (for *ca.* 1.5 hrs at GHSV = 1200 h⁻¹ rel. to 25°C and 1 atm) with minimal to no elemental sulfur slip upon returning to normal operating conditions. The mass balance calculations here were performed using GC measurements of product H₂S which have an associated relative error of *ca.* ±2.5%. When simulating the power disruption, sulfur formation from the Claus reaction was indicated in the first sample after the bed inlet temperature dropped below 200°C/390°F. In the adiabatic system, this represented a 38- to 53-minute window between loss of the tail gas reheater and sulfur production on the catalyst surface. While the size and nature of the reheater will also impact this timing, it is presumed that our findings provide a conservative estimate. Our time-on-stream while simulating no gas pre-heat corresponded to a power disruption time of *ca.* 1.8 hours. Finally, the temperature profiles across the catalyst bed before and after the simulated temperature event indicated no damage or loss in activity of the catalyst. This was further supported by the surface area analyses that were performed in the initial isothermal testing.

Implementation at HRO: TGU “Run Through”

Following the isothermal reactor studies, the LYB team concluded that this new concept was indeed viable and decided to move forward with implementation before the adiabatic study was complete with conservative parameters that could be adjusted later if required. The team reviewed the SIS modifications necessary to safely keep the TGU path open from the Claus units following a shutdown of the ILH enabling this “run through” concept to transpire. This required a method to adequately monitor the reaction activity across the entire catalyst bed. A concept used in traditional oil refining hydrotreating to monitor overall catalyst bed performance is weighted average bed temperature (WABT); it was concluded that this monitoring method would be the best approach (see Figure 16 for calculational method used for the 440 TGU). The DCS collects the temperature probe information of all the bed thermocouples and then calculates the WABT reporting to a new DCS tag. A process hazard analysis (PHA) was conducted to ensure the changes could be implemented safely focusing on deflagration prevention and determining the proper termination conditions for the “run through” operation.

Since the TGU ILH combustion air, natural gas and hydrogen streams all already had triple shutdown isolation (two dedicated SIS isolation valves and the SIS/DCS forced closure of the flow controller) deflagration potential was ruled out as a concern. The team chose a WABT of 410 °F for the alarm point for console operator response to manually close the TGU inlet valve to terminate the “run through” operation. It was decided that operator intervention to terminate was better suited than implementing an automated response for the feed valve closure so that readiness to switch can have proper evaluation. The SIS automated action on the feed valve closure to the tail gas unit upon shutdown of the ILH was removed from the Triconex SIS logic programing. By implementing these changes, both TGU's would now have the ability to continue to accept and process tail gas load from the Claus units following a corresponding ILH trip; providing more time to either shift the gas load from the Claus units to the other TGU or take other mitigations to eliminate or minimize the environmental impact. The changes were implemented into both TGU's in August 2022.



$$WABT = \frac{0.5 \times [TOP \text{ AVG Temp}_1 + 2(Mid \text{ AVG Temp}_2)]}{3} + \frac{0.5 \times [(Mid \text{ AVG Temp}_2 + 2(BTM \text{ AVG Temp}_3)]}{3}$$

Note: The TOP, MID and BTM level temperatures are averages of the four probes at that level.

Figure 16: Calculation method for weighted average bed temperature (WABT) on the 440 TGU hydrogenation reactor.

Actual “Run Through” Events

On December 23, 2022, South Texas was impacted by the freezing weather associated with Winter Storm Elliot. Being a Gulf Coast facility, HRO is not inherently designed to handle extreme cold weather events. Previous recent freeze events (such as Winter Storm Uri in February 2021) have led to protection improvements to help the site manage through such events. However, the 435 TGU sits on the west end of the HRO SRC where virtually all of the equipment has a northwestern exposure right next to the Ship Channel. When the cold front came through that day, it packed a powerful and long-lasting wind front that had a significant area residual heat (heat normally present from the surrounding equipment) removal effect that impacted the unit’s associated equipment, particularly the water handling equipment of the Quench and Amine sections. The loss of this residual area heat resulted in vulnerable critical unit instrumentation losing its functionality. At the time of the event, the ambient temperature was ~21°F so with no residual process heat in the vicinity, the instruments susceptible to freezing failed. Lost of instrumentation had already tripped the 435 Thermal Oxidizer when a sudden temporary power loss tripped the unit’s ILH combustion air blower resulting in a flame out shutdown of the ILH.

During normal operations, the tail gas reactor inlet is typically about 485°F with a corresponding outlet temperature ranging between 500-525°F. With the upset condition ongoing at the time, the 435 TGU reactor outlet temperature was hovering at ~495°F and the Claus unit processing load handled by the TGU was approximately 300 LT/D at the time of the 435 ILH trip. When the trip occurred, many other freeze condition emergency issues were occurring throughout the SRC and the entire refinery including the motor operator failure of the 435 TGU tail gas inlet valve MOV-1000. Therefore, the operating team decided to take full advantage of the “run through” concept to aid with all of their issues before switching the Claus tail gas load over to the operating U-440 TGU. The reactor took approximately 90 minutes to reach the target stop temperature of 410°F as shown in Figure 17. The Operators were able to safely manually close the MOV-1000 during this time and safely transition the gas load from the 433/434 Claus units to the other online TGU. During the event, the SO₂ concentrations of both thermal oxidizer stacks stayed well below their permit limits of 250 ppmv. No long-term problems have been observed in the catalyst bed’s performance as a result of this event.

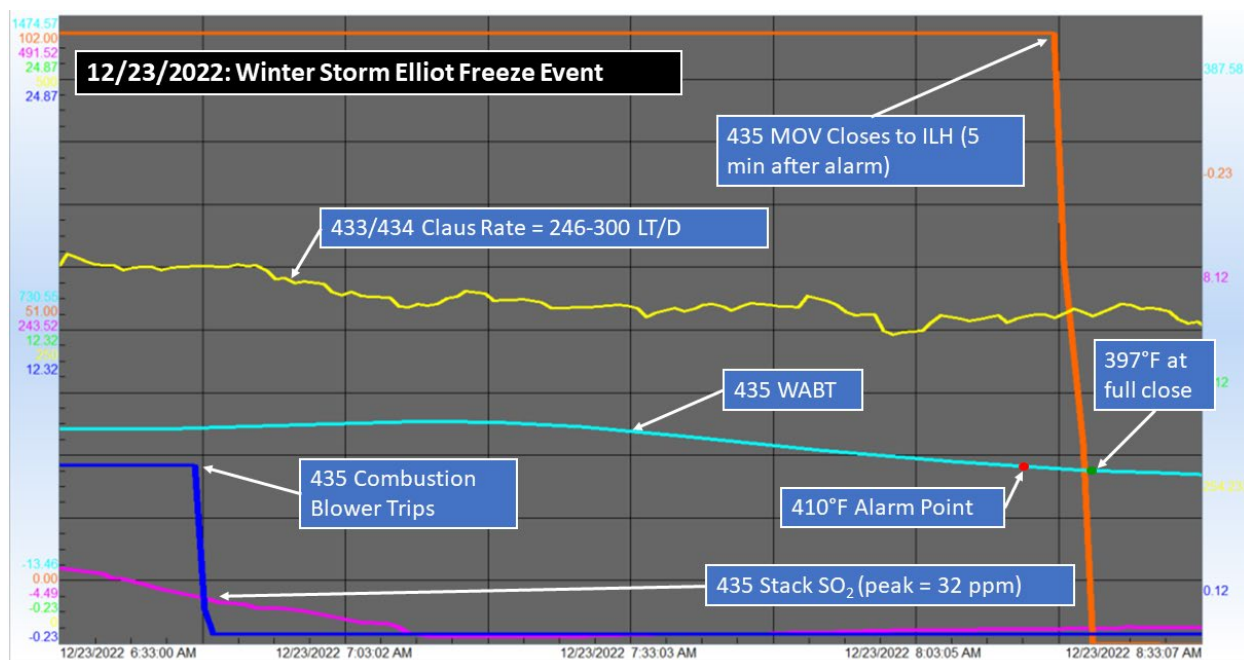


Figure 17: December 23, 2022 freeze event 435 TGU “run through” data.

On April 21, 2024, a second “run through” event occurred that was caused by unexpected problems during the tail gas load transfer for a scheduled shutdown of the 435 Tail Gas Unit for unplanned maintenance work. While in the process of transferring the tail gas load from the 435 TGU to the 440 TGU, the 440 ILH suffered a sudden and unexpected ILH flame out trip event. At the time of the trip, the 435 TGU inlet MOV-1000 was only 5% open with essentially the entire SRC Claus unit tail gas load routing through to the 440 TGU. Upon the 440 ILH trip, the Operations team had to appropriately “undo” the tail gas transfer in a manner that would not disrupt Claus unit operations and/or result in a trip of the 435 TGU ILH. Allowing the “run through” to progress on

the 440 TGU provided sufficient time for the operations team to move the entire SRC tail gas load safely unto to the 435 TGU. The tail gas “run through” on the 440 TGU lasted 38 minutes with the Claus unit load at the start of the event being ~487 LT/D. After the load was shifted back to 435 TGU and the “run through” operation ceased, the Operations team was able to trouble shoot to determine the cause of the 440 TGU trip and then proceed with its safe relighting. Upon return of the 440 TGU operation, tail gas load was then able to be safely/properly transferred back onto the 440 TGU without further incident on the ILH. All total this this took approximately 100 minutes for the operations team to complete.

While in the 440 TGU “run through” mode, Operations monitored the WABT across the tail gas reactor and this temperature never fell below 490°F allowing full conversion of sulfur species to the H₂S for amine capture without exceeding the SO₂ limit on the thermal oxidizer; in fact, there virtually was no change in the stack SO₂ concentrations (see Figure 18). This event was the first true verification that allowing tail gas to “run through” an unlit ILH can indeed provide full conversion of sulfur species with sustained reactor WABT; providing precious time for the Operations team to rectify the situation. Additionally, throughout the entire event including the load transfer, trip incident, 440 TGU "run through" operation and 440 unit restart; no further refinery rate adjustments were needed to “manage” the event. Having the “run through” capability provided impact results that emulated as if the incident never happened!

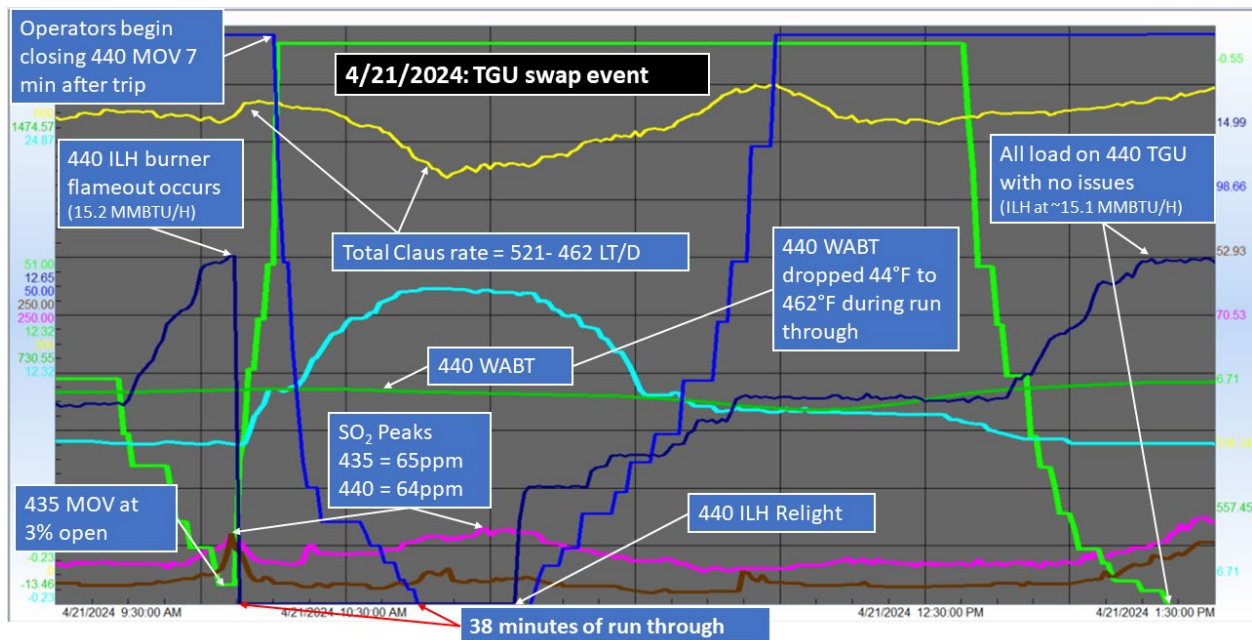


Figure 18: April 21, 2024 maintenance event 440 TGU “run through” data.

Historical HRO Trip Events

To fully appreciate the overall step change in performance obtained by implementing this concept, comparison to the outcomes of similar historical events needs to be made. Prior to implementing

the concept change, the Triconex SIS logic utilized in both TGU's would automatically close the Claus unit tail gas inlet feed valves to the ILH immediately upon an ILH trip event. This would lead to a rapid shift of gas load from the Claus unit(s) to be either shifted to the other on-line TGU or diverted directly to thermal oxidizers if the other TGU is not available while the operations team went to restart the TGU(s). Additionally, these actions have led to cascading shutdowns of the online Claus units due to backpressure on the units. By not immediately diverting the gas to thermal oxidizer or to the other online TGU, operations can shift the gas between the units and take the time to safely stabilize the units while shifting the gas loads. Figure 19 shows the data from a momentary electrical power disruption that occurred on June 18, 2019 tripping the 440 TGU ILH. This event happened under the old SIS logic scheme where the 440 ILH inlet valve was automatically and immediately closed forcing all of the Claus tail gas to the 435 TGU. The resultant impact was stack SO₂ concentration spikes on both thermal oxidizers with the highest value peaking at over 4300 ppmv and the entire event lasting ~40 minutes with SO₂ elevated to these levels. Additionally, what is not shown is that the CO concentrations on both stacks also suffered permit limit exceedances as a result.

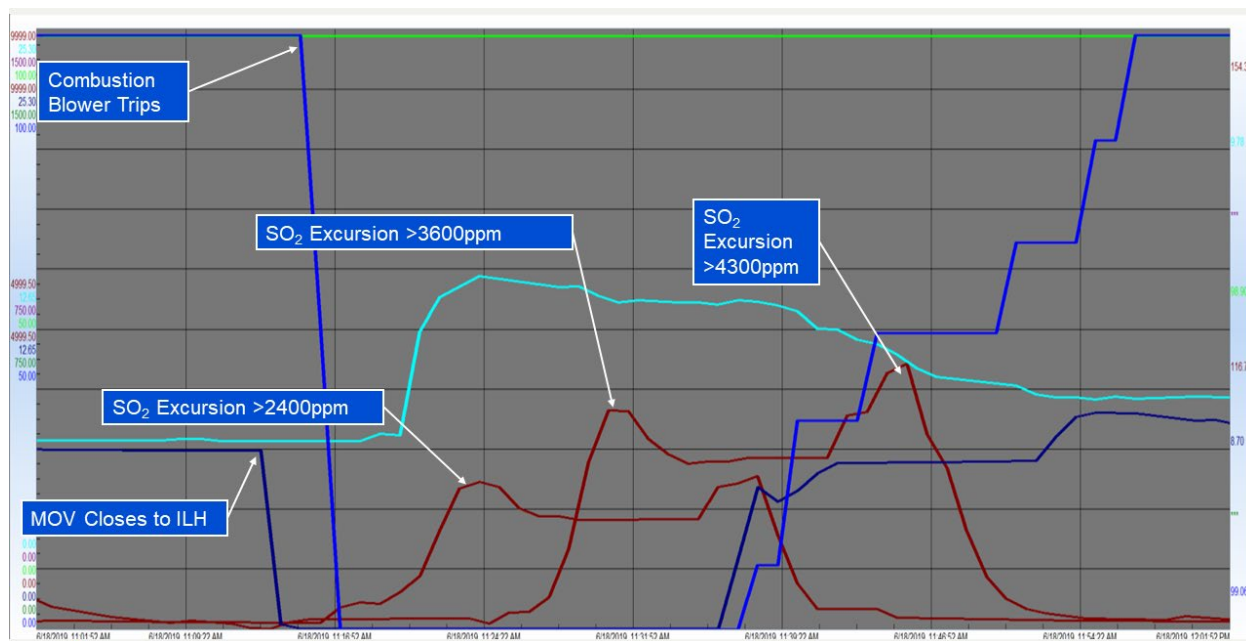


Figure 19: June 18, 2019 electrical power disruption 440 TGU ILH trip event data.

Conclusions

The ASRL tail gas conversion catalyst study contracted by Houston Refining LP (LyondellBasell) using Topsoe TK-220 and TK-222 catalyst that are currently deployed in the Houston Refinery Sulfur Recovery Facility tail gas units (TGU's) demonstrates that sulfur species conversion to H₂S is sustainable for a period of time with tail gas feed temperatures at normal Claus unit final condenser outlet temperature (~275°F) until the TGU catalyst weighted average bed temperature (WABT) falls to 400°F (205°C). This finding allowed Houston Refining to institute an entirely

new operations response philosophy to TGU inline heater (ILH) trip off events that has thus far negated the typical negative environmental impacts associated with these upset events. By allowing the un-reheated Claus tail gas to continue flowing through the TGU after the ILH has tripped off (the “run through” concept), significant time is now allotted to the operating team to have a greatly improved, systematic, safe upset response that has eliminated the SO₂ excursions that were associated with the automated streams switching previously executed by the Triconex safety instrumented systems (SIS). This change also provides a broader window of operation to manage various unplanned scenarios known for causing major reliability impacts to the refinery operation. Finally, it has shown minimal to no reliability impacts to the equipment and the tail gas catalyst following these events. ■

References

[1] Clark P.D., Dowling N.I., Huang M., Okemona O., Butlin G.D., Hou R., Kijlstra W.S., Studies on sulfate formation during the conversion of H₂S and SO₂ to sulfur over activated alumina, *Applied Catalysis A: General*, 235 (2002), 61-69.

[2] Weekman V.W., Laboratory reactors and their limitations, *AIChE Journal*, Vol. 20, No. 5 (1974), 833-840.

Note the references 3-7 are not intended to be an exhaustive list of references on adiabatic reactors in the literature.

[3] Schmidt J.P., Mickley H.S., Grotch S.L., Use of adiabatic experiments for kinetic studies in fixed catalyst beds, *AIChE Journal*, Vol. 10, No. 2 (1964), 149-154.

[4] de Klerk A., Adiabatic laboratory reactor design and verification, *Ind. Eng. Chem. Res.*, Vol. 44, No. 25 (2005), 9440-9445.

[5] Perego C., Peratello S., Experimental methods in catalytic kinetics, *Catalysis Today*, Volume 52 (1999), 133-145.

[6] Mashapa T.N., de Klerk A., Solid phosphoric acid catalysed conversion of oxygenate containing Fischer-Tropsch naphtha, *Applied Catalysis A: General*, 332 (2007), 200-208.

[7] Chatterjee S., Houlding T.K., Doluda V.Y., Molchanov V.P., Matveeva V.G., Rebrov E.V., Thermal behaviour of a catalytic packed-bed milli-reactor operated under radio frequency, *Ind. Eng. Chem. Res.*, Vol. 56 (2017), 13273-13280.

About the Authors



Philip J. Oberbroeckling, P.E. is currently the Technology Integration Manager responsible for the new processing technology integration of the future sustainability projects into the LyondellBasell Houston Refinery site. Over Philip's 34 years of service in the oil refining industry, he has held numerous engineering and management positions in Technical, HSES, and Operations including 5-year tenure as the Operations Superintendent of the Houston Refinery Sulfur Recovery Complex (SRC), the Chief Engineer for the Houston SRC 2011-2013 Rebuild and Expansion Project, Technical Consultant to the Berre France Refinery Tail Gas Unit Project and the Process Technical Manager for the entire Houston Refinery. Before LyondellBasell, Philip held engineering positions for five years with Conoco Inc. at their Ponca City, OK engineering offices and at their oil refinery in Billings, MT. Philip holds a Bachelor of Science degree in Chemical Engineering from Iowa State University and is a registered Professional Engineer in Montana and Texas. Philip has authored 43 conference papers and presentations on sulfur recovery and oil refining topics. Philip is a member of the Brimstone Sulfur Recovery Symposium Technical Advisory Committee, was a charter member and Task-Group Chairman for the API 565 Standards Committee on SRU Thermal Reactors until its publishing in 2022, a member of the Amine Best Practices Group, a member of the AIChE and he is the Founder, President, and member of the Mr./Ms. Sulfur Club.



Amber L. Hans currently the Sulfur Recovery Unit Process Engineer at LyondellBasell Houston Refinery site. Prior to joining the Houston Refinery, Amber, has worked in industry for 7+ years with previous Production and Process Engineering roles in Polyethylene Manufacturing at LyondellBasell and Dow Chemical Company. Amber has a Bachelor of Science degree in Chemical Engineering from Iowa State University.



Craig J. Moody is currently the Sulfur Recovery Operations Specialist responsible for day to day operations for the SRU as well as execution and planning of all projects outages and maintenance at the SRU. Craig has 14 years of experience in refining as an Operator, Console Operator, and Supervisor responsible for the SRU, Utilities, Lubes and Delayed Coker Units prior to his current role. Craig has a Bachelor of Arts degree in Finance from The University of Texas at Austin.



Christopher B. Lavery is currently a Project Manager and Research Scientist at Alberta Sulphur Research Ltd. Since joining ASRL in 2013, Dr. Lavery has worked in various areas of process chemistry that relate to sulfur recovery in the oil and natural gas industry. Most of his research efforts are focused on the thermal and catalytic stages of the modified Claus process and tail gas treatment. However, Dr. Lavery also has research interests in corrosion, adsorption, and synthetic chemistry.



Robert A. Marriott is currently the Director of Research at Alberta Sulphur Research Ltd. and a Professor at the University of Calgary. Dr. Marriott's academic research is performed through the ASRL Research Chair in Applied Sulfur Chemistry which works in full collaboration with ASRL researchers. His interests include high-pressure reservoir chemistry, high-pressure adsorption, sour/acid gas phase behavior, sulfur recovery, corrosion, sulfur product handling and process chemistry. He has published more than 80 manuscripts and given over 50 talks at international venues.

Special Thanks to Topsoe for sponsoring the technical paper.

Appendix

Table A1: GC data collected over the course of the 72-hour test consisting of three (3) temperature cycles between 260°C/500°F and 135°C/275°.

Time (min.)	T_{bed} (°C)	N ₂	H ₂ S	SO ₂	CO ₂	CO	H ₂	H ₂ O	S ₈	Outlet H ₂ S (mmol/min)	
		mols / 100 mols of feed								Measured	Expected
Feed		50.54	0.60	0.20	1.81	0.31	2.43	44.08	0.03		
25	260	50.54	1.71	0.00	2.09	0.00	1.33	44.07	-0.08	0.596	0.362
50	260	50.54	1.79	0.00	2.16	0.00	1.37	43.94	-0.09	0.624	0.362
75	260	50.54	1.71	0.00	2.17	0.00	1.40	44.06	-0.08	0.595	0.362
100	260	50.54	1.87	0.00	2.20	0.00	0.00	45.34	-0.10	0.653	0.362
125	260	50.54	1.27	0.00	2.19	0.00	0.00	43.41	-0.03	0.442	0.362
150	260	50.54	1.20	0.00	2.20	0.00	0.00	43.48	-0.02	0.418	0.362
175	250	50.54	1.10	0.00	2.20	0.00	2.17	41.42	-0.01	0.382	0.362
200	240	50.54	0.99	0.00	2.18	0.00	2.11	45.47	0.01	0.345	0.362
225	230	50.54	0.97	0.00	2.19	0.00	2.16	45.35	0.01	0.338	0.362
250	220	50.54	0.93	0.00	2.19	0.00	2.16	45.47	0.01	0.323	0.362
275	210	50.54	0.92	0.00	2.19	0.00	2.19	45.46	0.01	0.321	0.362
300	200	50.54	0.79	0.00	2.17	0.00	2.26	45.58	0.03	0.273	0.362
325	190	50.54	0.92	0.00	2.19	0.01	2.37	45.44	0.01	0.322	0.362
350	180	50.54	0.64	0.00	2.17	0.01	2.36	45.92	0.05	0.222	0.362
375	170	50.54	0.56	0.00	2.14	0.03	2.41	45.97	0.06	0.195	0.362
400	160	50.54	0.48	0.00	2.14	0.04	2.46	46.08	0.07	0.166	0.362
425	150	50.54	0.65	0.00	2.12	0.12	2.57	45.89	0.05	0.225	0.362
450	140	50.54	0.47	0.00	2.07	0.13	2.55	46.27	0.07	0.163	0.362
475	135	50.54	0.39	0.00	2.04	0.14	2.50	46.36	0.08	0.136	0.362
500	135	50.54	0.42	0.00	2.11	0.17	2.54	46.23	0.08	0.145	0.362
525	135	50.54	0.43	0.00	2.04	0.16	2.53	46.28	0.08	0.149	0.362
550	135	50.54	0.33	0.00	2.04	0.13	2.54	46.36	0.09	0.115	0.362
575	145	50.54	0.43	0.00	2.06	0.14	2.58	46.25	0.08	0.148	0.362
600	155	50.54	0.42	0.00	2.10	0.09	2.53	46.36	0.08	0.147	0.362
625	165	50.54	0.44	0.00	2.08	0.05	2.48	46.32	0.07	0.154	0.362
650	175	50.54	0.51	0.00	2.16	0.03	2.43	46.21	0.07	0.179	0.362
675	185	50.54	0.65	0.00	2.17	0.01	2.42	45.98	0.05	0.226	0.362
700	195	50.54	0.79	0.00	2.19	0.01	2.28	45.95	0.03	0.276	0.362
725	205	50.54	0.97	0.00	2.19	0.00	2.09	45.72	0.01	0.338	0.362
750	215	50.54	1.35	0.00	2.21	0.00	1.91	45.18	-0.04	0.471	0.362
775	225	50.54	1.64	0.00	2.21	0.00	1.60	44.86	-0.08	0.573	0.362
800	235	50.54	2.24	0.00	2.21	0.00	1.33	43.98	-0.15	0.779	0.362
825	245	50.54	2.38	0.00	2.18	0.00	0.76	43.92	-0.17	0.827	0.362
850	255	50.54	3.43	0.00	2.15	0.00	0.55	42.08	-0.30	1.195	0.362
875	260	50.54	3.07	0.00	2.19	0.00	0.26	42.32	-0.25	1.068	0.362
900	260	50.54	1.97	0.00	2.18	0.00	1.20	41.98	-0.12	0.685	0.362
925	260	50.54	1.18	0.00	2.24	0.00	2.10	43.57	-0.02	0.411	0.362
950	260	50.54	1.05	0.00	2.19	0.00	2.10	45.30	0.00	0.365	0.362
975	260	50.54	1.06	0.00	2.20	0.00	1.98	45.43	0.00	0.370	0.362
1000	260	50.54	1.02	0.00	2.16	0.00	2.02	45.20	0.00	0.356	0.362
1025	260	50.54	1.01	0.00	2.12	0.00	2.04	45.27	0.00	0.352	0.362
1050	260	50.54	1.05	0.00	2.18	0.00	2.02	45.30	0.00	0.364	0.362
1075	260	50.54	1.03	0.00	2.20	0.00	1.85	45.43	0.00	0.359	0.362

1100	260	50.54	1.03	0.00	2.16	0.00	2.01	44.98	0.00	0.358	0.362
1125	260	50.54	1.02	0.00	2.15	0.00	2.02	45.26	0.00	0.354	0.362
1150	250	50.54	0.98	0.00	2.14	0.00	2.09	45.26	0.01	0.340	0.362
1175	240	50.54	1.03	0.00	2.15	0.00	2.10	45.32	0.00	0.360	0.362
1200	230	50.54	0.95	0.00	2.16	0.00	2.12	45.39	0.01	0.330	0.362
1225	220	50.54	0.92	0.00	2.17	0.00	2.13	45.43	0.01	0.321	0.362
1250	210	50.54	1.07	0.00	2.23	0.00	2.11	45.35	0.00	0.372	0.362
1275	200	50.54	0.77	0.00	2.09	0.00	2.37	45.34	0.03	0.268	0.362
1300	190	50.54	0.76	0.00	2.18	0.01	2.29	45.89	0.04	0.264	0.362
1325	180	50.54	0.61	0.00	2.12	0.01	2.32	45.87	0.05	0.213	0.362
1350	170	50.54	0.54	0.00	2.12	0.02	2.36	45.94	0.06	0.189	0.362
1375	160	50.54	0.46	0.00	2.13	0.03	2.44	46.04	0.07	0.158	0.362
1400	150	50.54	0.50	0.00	2.09	0.09	2.46	46.13	0.07	0.173	0.362
1425	140	50.54	0.45	0.00	2.26	0.11	2.50	46.17	0.07	0.155	0.362
1450	135	50.54	0.46	0.00	2.04	0.15	2.51	46.21	0.07	0.160	0.362
1475	135	50.54	0.45	0.00	2.04	0.15	2.51	46.24	0.07	0.156	0.362
1500	135	50.54	0.31	0.00	2.03	0.10	2.47	46.42	0.09	0.109	0.362
1525	135	50.54	0.37	0.00	2.03	0.13	2.54	46.24	0.08	0.131	0.362
1550	145	50.54	0.59	0.00	2.32	0.22	2.66	46.00	0.06	0.207	0.362
1575	155	50.54	0.51	0.00	2.12	0.11	2.54	46.38	0.07	0.176	0.362
1600	165	50.54	0.44	0.00	2.14	0.05	2.47	46.35	0.08	0.152	0.362
1625	175	50.54	0.51	0.00	2.16	0.03	2.47	46.16	0.07	0.176	0.362
1650	185	50.54	0.70	0.00	2.19	0.03	2.36	46.08	0.04	0.243	0.362
1675	195	50.54	0.78	0.00	2.20	0.01	2.23	45.93	0.03	0.271	0.362
1700	205	50.54	1.07	0.00	2.21	0.00	2.16	45.48	0.00	0.371	0.362
1725	205	50.54	1.10	0.00	2.28	0.01	2.29	45.19	-0.01	0.384	0.362
1750	205	50.54	1.10	0.00	2.18	0.00	1.98	45.66	-0.01	0.383	0.362
1775	205	50.54	1.26	0.00	2.20	0.00	2.14	44.86	-0.03	0.438	0.362
1800	205	50.54	1.13	0.00	2.20	0.00	1.92	45.46	-0.01	0.393	0.362
1825	205	50.54	1.19	0.00	2.19	0.01	1.91	45.06	-0.02	0.414	0.362
1850	205	50.54	1.33	0.00	2.20	0.01	1.97	44.83	-0.04	0.462	0.362
1875	215	50.54	1.72	0.00	2.20	0.01	1.88	44.62	-0.09	0.600	0.362
1900	215	50.54	1.53	0.00	2.20	0.00	1.62	44.90	-0.06	0.531	0.362
1925	215	50.54	1.61	0.00	2.20	0.04	1.56	44.42	-0.07	0.562	0.362
1950	215	50.54	1.57	0.00	2.19	0.00	1.48	44.44	-0.07	0.548	0.362
1975	225	50.54	1.76	0.00	2.20	0.00	1.36	44.24	-0.09	0.613	0.362
2000	225	50.54	1.76	0.00	2.22	0.00	1.27	44.11	-0.09	0.614	0.362
2025	225	50.54	2.62	0.00	2.24	0.00	1.41	42.95	-0.20	0.911	0.362
2050	225	50.54	2.27	0.00	2.18	0.00	0.87	44.05	-0.15	0.790	0.362
2075	235	50.54	1.90	0.00	2.31	0.00	2.50	41.85	-0.11	0.661	0.362
2100	235	50.54	1.61	0.00	2.26	0.00	2.04	45.41	-0.07	0.562	0.362
2125	235	50.54	1.17	0.00	2.18	0.00	1.84	45.31	-0.02	0.408	0.362
2150	235	50.54	1.08	0.00	2.17	0.00	1.96	44.96	0.00	0.376	0.362
2175	245	50.54	1.14	0.00	2.19	0.00	1.99	45.09	-0.01	0.398	0.362
2200	245	50.54	1.29	0.00	2.26	0.00	2.06	44.91	-0.03	0.449	0.362
2225	245	50.54	1.23	0.00	2.22	0.00	2.02	45.14	-0.02	0.427	0.362
2250	245	50.54	1.02	0.00	2.18	0.00	2.00	45.28	0.00	0.355	0.362
2275	255	50.54	1.08	0.00	2.17	0.00	2.02	45.19	-0.01	0.377	0.362
2300	255	50.54	1.06	0.00	2.23	0.00	1.39	45.85	0.00	0.370	0.362
2325	255	50.54	0.91	0.00	2.13	0.00	1.87	44.43	0.02	0.317	0.362
2350	255	50.54	1.08	0.00	2.16	0.00	2.05	44.95	-0.01	0.377	0.362

2375	260	50.54	1.04	0.00	2.14	0.00	2.09	45.24	0.00	0.363	0.362
2400	260	50.54	1.09	0.00	2.28	0.00	1.82	45.54	-0.01	0.381	0.362
2425	260	50.54	1.02	0.00	2.19	0.00	1.91	45.02	0.00	0.356	0.362
2450	260	50.54	1.09	0.00	2.16	0.00	2.02	45.01	-0.01	0.380	0.362
2475	260	50.54	1.04	0.00	2.15	0.00	2.06	45.22	0.00	0.361	0.362
2500	260	50.54	1.01	0.00	2.18	0.00	2.03	45.36	0.00	0.351	0.362
2525	260	50.54	1.03	0.00	2.32	0.00	2.26	45.05	0.00	0.358	0.362
2550	260	50.54	1.02	0.00	2.19	0.00	1.98	45.71	0.00	0.356	0.362
2575	260	50.54	1.19	0.00	2.29	0.00	2.15	44.92	-0.02	0.415	0.362
2600	260	50.54	1.01	0.00	2.18	0.00	2.05	45.46	0.00	0.353	0.362
2625	260	50.54	1.04	0.00	2.18	0.00	2.14	45.20	0.00	0.361	0.362
2650	250	50.54	0.95	0.00	2.15	0.00	2.07	45.51	0.01	0.331	0.362
2675	240	50.54	0.97	0.00	2.21	0.00	2.07	45.38	0.01	0.339	0.362
2700	230	50.54	0.92	0.00	2.15	0.00	2.16	45.35	0.02	0.320	0.362
2725	220	50.54	0.93	0.00	2.19	0.00	2.15	45.50	0.01	0.325	0.362
2750	210	50.54	0.89	0.00	2.19	0.00	2.18	45.47	0.02	0.311	0.362
2775	200	50.54	0.88	0.00	2.20	0.00	2.25	45.48	0.02	0.307	0.362
2800	190	50.54	0.86	0.00	2.22	0.01	2.39	45.48	0.02	0.301	0.362
2825	180	50.54	0.75	0.00	2.16	0.01	2.37	45.84	0.04	0.263	0.362
2850	170	50.54	0.65	0.00	2.17	0.03	2.39	45.90	0.05	0.228	0.362
2875	160	50.54	0.64	0.00	2.19	0.06	2.54	45.81	0.05	0.222	0.362
2900	150	50.54	0.56	0.00	2.10	0.10	2.49	46.20	0.06	0.194	0.362
2925	140	50.54	0.41	0.00	2.05	0.10	2.47	46.27	0.08	0.143	0.362
2950	135	50.54	0.42	0.00	2.05	0.15	2.55	46.17	0.08	0.147	0.362
2975	135	50.54	0.44	0.00	2.05	0.16	2.47	46.38	0.08	0.152	0.362
3000	135	50.54	0.40	0.00	2.06	0.15	2.53	46.19	0.08	0.140	0.362
3025	135	50.54	0.36	0.00	2.04	0.13	2.50	46.37	0.08	0.126	0.362
3050	135	50.54	0.49	0.00	2.07	0.20	2.49	46.20	0.07	0.172	0.362
3075	135	50.54	0.44	0.00	2.06	0.17	2.55	46.16	0.08	0.153	0.362
3100	135	50.54	0.40	0.00	2.06	0.16	2.53	46.34	0.08	0.138	0.362
3125	135	50.54	0.45	0.00	2.03	0.18	2.49	46.30	0.07	0.157	0.362
3150	145	50.54	0.42	0.00	2.09	0.14	2.57	46.17	0.08	0.145	0.362
3175	155	50.54	0.45	0.00	2.10	0.10	2.53	46.32	0.07	0.158	0.362
3200	165	50.54	0.51	0.00	2.13	0.07	2.53	46.21	0.07	0.177	0.362
3225	175	50.54	0.54	0.00	2.14	0.04	2.46	46.23	0.06	0.189	0.362
3250	185	50.54	0.69	0.00	2.18	0.03	2.39	46.02	0.04	0.240	0.362
3275	195	50.54	0.88	0.00	2.20	0.01	2.28	45.81	0.02	0.306	0.362
3300	205	50.54	1.08	0.00	2.20	0.01	2.13	45.57	0.00	0.375	0.362
3325	205	50.54	1.17	0.00	2.20	0.01	2.06	45.26	-0.02	0.408	0.362
3350	205	50.54	1.28	0.00	2.20	0.01	2.02	45.08	-0.03	0.447	0.362
3375	205	50.54	1.28	0.00	2.19	0.01	2.03	45.00	-0.03	0.444	0.362
3400	205	50.54	1.36	0.00	2.17	0.01	1.96	44.99	-0.04	0.474	0.362
3425	205	50.54	1.32	0.00	2.18	0.01	1.90	44.98	-0.04	0.461	0.362
3450	205	50.54	1.29	0.00	2.19	0.01	1.88	44.93	-0.03	0.449	0.362
3475	215	50.54	1.56	0.00	2.20	0.01	1.74	44.77	-0.06	0.543	0.362
3500	215	50.54	1.75	0.00	2.19	0.01	1.65	44.40	-0.09	0.609	0.362
3525	215	50.54	1.63	0.00	2.17	0.02	1.62	44.38	-0.07	0.569	0.362
3550	215	50.54	1.63	0.00	2.20	0.02	1.53	44.43	-0.07	0.568	0.362
3575	225	50.54	1.97	0.00	2.20	0.02	1.59	43.89	-0.12	0.685	0.362
3600	225	50.54	1.72	0.00	2.20	0.01	1.39	44.43	-0.08	0.598	0.362
3625	225	50.54	2.05	0.00	2.19	0.01	1.45	43.70	-0.13	0.713	0.362

3650	225	50.54	2.62	0.00	2.24	0.00	1.31	43.34	-0.20	0.911	0.362
3675	235	50.54	2.19	0.00	2.18	0.00	0.99	43.84	-0.14	0.763	0.362
3700	235	50.54	1.44	0.00	2.07	0.00	1.91	43.11	-0.05	0.501	0.362
3725	235	50.54	1.27	0.00	2.19	0.00	1.76	45.07	-0.03	0.443	0.362
3750	235	50.54	1.27	0.00	2.43	0.00	3.65	42.95	-0.03	0.441	0.362
3775	245	50.54	1.09	0.00	2.19	0.00	2.13	47.50	-0.01	0.380	0.362
3800	245	50.54	1.26	0.00	2.56	0.01	3.55	43.72	-0.03	0.438	0.362
3825	245	50.54	1.19	0.00	2.21	0.00	1.87	47.54	-0.02	0.414	0.362
3850	245	50.54	1.22	0.00	2.19	0.00	2.03	44.81	-0.02	0.424	0.362
3875	255	50.54	1.22	0.00	2.22	0.00	2.03	45.08	-0.02	0.426	0.362
3900	255	50.54	1.16	0.00	2.20	0.00	2.06	45.09	-0.02	0.405	0.362
3925	255	50.54	1.12	0.00	2.20	0.00	2.08	45.18	-0.01	0.390	0.362
3950	255	50.54	1.05	0.00	2.13	0.00	2.16	45.21	0.00	0.366	0.362
3975	260	50.54	1.01	0.00	2.16	0.00	2.06	45.51	0.00	0.353	0.362
4000	260	50.54	0.99	0.00	2.18	0.00	1.74	45.67	0.01	0.346	0.362
4025	260	50.54	1.00	0.00	2.09	0.00	1.91	44.93	0.00	0.349	0.362
4050	260	50.54	1.03	0.00	2.13	0.00	1.66	45.45	0.00	0.358	0.362
4075	260	50.54	1.01	0.00	2.07	0.00	1.63	45.07	0.00	0.351	0.362
4100	260	50.54	1.09	0.00	2.18	0.00	2.19	44.38	-0.01	0.381	0.362
4125	260	50.54	0.98	0.00	2.15	0.00	1.97	45.65	0.01	0.343	0.362
4150	260	50.54	1.14	0.00	2.18	0.00	2.08	45.02	-0.01	0.397	0.362
4175	260	50.54	1.03	0.00	2.17	0.00	2.13	45.26	0.00	0.358	0.362
4200	260	50.54	1.23	0.00	2.32	0.00	2.03	45.26	-0.02	0.427	0.362
4225	260	50.54	1.08	0.00	2.20	0.00	2.19	45.03	-0.01	0.378	0.362
4250	256	50.54	0.94	0.00	2.18	0.00	2.07	45.59	0.01	0.328	0.362
4275	244	50.54	0.84	0.00	2.15	0.00	2.16	45.42	0.03	0.292	0.362
4300	231	50.54	0.73	0.00	2.16	0.00	2.13	45.72	0.04	0.254	0.362
4325	217	50.54	0.66	0.00	2.12	0.00	2.34	45.54	0.05	0.232	0.362
4350	205	50.54	0.81	0.00	2.29	0.01	2.37	45.71	0.03	0.282	0.362
4375	193	50.54	0.55	0.00	2.14	0.01	2.42	45.97	0.06	0.192	0.362
4400	182	50.54	0.44	0.00	2.57	0.13	3.27	45.35	0.08	0.152	0.362
4425	171	50.54	0.39	0.00	2.12	0.02	2.54	47.38	0.08	0.134	0.362
4450	162	50.54	0.34	0.00	2.21	0.22	2.70	46.23	0.09	0.118	0.362
4475	152	50.54	0.28	0.00	2.05	0.05	2.53	46.66	0.09	0.099	0.362
4500	144	50.54	0.37	0.00	2.07	0.11	2.53	46.36	0.08	0.130	0.362
4525	138	50.54	0.35	0.00	1.98	0.31	2.59	46.31	0.09	0.121	0.362
4550	134	50.54	0.33	0.00	2.30	0.12	2.82	46.17	0.09	0.115	0.362